



HAL
open science

Recent Progress in Metal-Catalyzed [2+2+2] Cycloaddition Reactions

Pascal Matton, Steve Huvelle, Mansour Haddad, Phannarath Phansavath,
Virginie Ratovelomanana-Vidal

► **To cite this version:**

Pascal Matton, Steve Huvelle, Mansour Haddad, Phannarath Phansavath, Virginie Ratovelomanana-Vidal. Recent Progress in Metal-Catalyzed [2+2+2] Cycloaddition Reactions. *Synthesis: Journal of Synthetic Organic Chemistry*, 2021, 54 (01), pp.4 - 32. 10.1055/s-0040-1719831 . hal-03854060

HAL Id: hal-03854060

<https://hal.science/hal-03854060>

Submitted on 23 Nov 2022

HAL is a multi-disciplinary open access archive for the deposit and dissemination of scientific research documents, whether they are published or not. The documents may come from teaching and research institutions in France or abroad, or from public or private research centers.

L'archive ouverte pluridisciplinaire **HAL**, est destinée au dépôt et à la diffusion de documents scientifiques de niveau recherche, publiés ou non, émanant des établissements d'enseignement et de recherche français ou étrangers, des laboratoires publics ou privés.

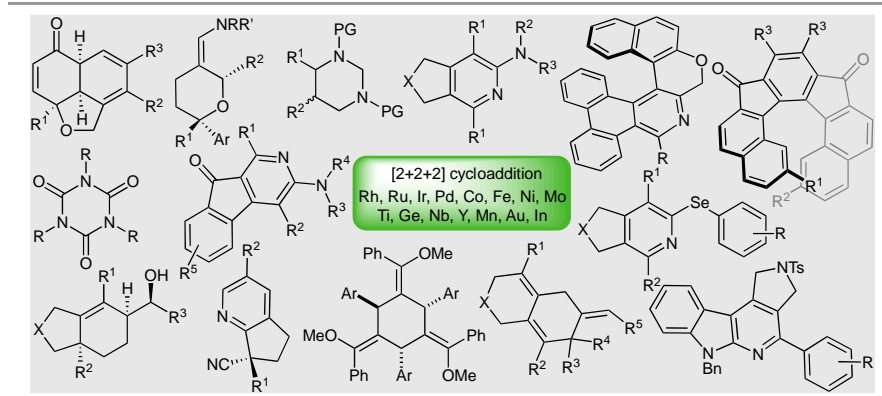
Recent Progress in Metal-Catalyzed [2+2+2] Cycloaddition Reactions

Pascal Matton^aSteve Huvelle^aMansour Haddad^aPhannarath Phansavath^aVirginie Ratovelomanana-Vidal^{a*}

^a PSL University, Chimie ParisTech-CNRS, Institute of Chemistry for Life & Health Sciences, CSB2D Team, 11 rue Pierre et Marie Curie, 75005 Paris, France.

virginie.vidal@chimieparitech.psl.eu

[Click here to insert a dedication.](#)



Received:

Accepted:

Published:

DOI:

online:

1. Introduction

Abstract Metal-catalyzed [2+2+2] cycloaddition is a powerful tool that allows rapid construction of functionalized 6-membered carbo- and heterocycles in a single step through an atom-economical process with high functional group tolerance. The reaction is usually regio- and chemoselective although selectivity issues can still be challenging for intermolecular reactions involving the cross-[2+2+2] cycloaddition of two or three different alkynes and various strategies have been developed to attain high selectivities. Furthermore, enantioselective [2+2+2] cycloaddition is an efficient means to create central, axial and planar chirality and a variety of chiral organometallic complexes can be used for the asymmetric transition metal-catalyzed inter- and intramolecular reaction. This review summarizes the recent advances in the field of [2+2+2] cycloaddition.

- 1 Introduction
- 2 Formation of Carbocycles
 - 2.1 Intermolecular Reactions
 - 2.1.1 Cyclotrimerization of Alkynes
 - 2.1.2 [2+2+2] Cycloaddition of Two Different Alkynes
 - 2.1.3 [2+2+2] Cycloaddition of Alkynes/Alkenes with Alkenes/Enamides
 - 2.2 Partially Intramolecular [2+2+2] Cycloaddition Reactions
 - 2.2.1 Rhodium-Catalyzed [2+2+2] Cycloaddition
 - 2.2.2 Molybdenum-Catalyzed [2+2+2] Cycloaddition
 - 2.2.3 Cobalt-Catalyzed [2+2+2] Cycloaddition
 - 2.2.4 Ruthenium-Catalyzed [2+2+2] Cycloaddition
 - 2.2.5 Other Metal-Catalyzed [2+2+2] Cycloaddition
- 2.3 Totally Intramolecular [2+2+2] Cycloaddition Reactions
- 3 Formation of Heterocycles
 - 3.1 Cycloaddition of Alkynes with Nitriles
 - 3.2 Cycloaddition of 1,6-Diynes with Cyanamides
 - 3.3 Cycloaddition of 1,6-Diynes with Selenocyanates
 - 3.4 Cycloaddition of Imines with Allenes or Alkenes
 - 3.5 Cycloaddition of (Thio)Cyanates and Isocyanates
 - 3.6 Cycloaddition of 1,3,5-Triazines with Allenes
 - 3.7 Cycloaddition of Aldehydes with Enynes or Allenes/Alkenes
 - 3.8 Totally Intramolecular [2+2+2] Cycloaddition Reactions
- 4 Conclusion

Key words cycloaddition, cyclotrimerization, transition metal, arenes, heterocycles, polycycles, asymmetric catalysis, alkynes, homogeneous catalysis

One of the most efficient routes to access highly substituted six-membered ring systems undoubtedly relies on transition metal-catalyzed [2+2+2] cycloaddition reaction of unsaturated motifs. Among them, cyclotrimerization of alkynes is one of the most useful and general method to produce benzene rings. After Berthelot discovered the thermal cyclotrimerization of acetylene to benzene in 1866,¹ Reppe and Schweckendiek² reported the first transition metal-catalyzed [2+2+2] cycloaddition reaction of alkynes using a nickel complex in 1948. Rothwell and co-workers were the first to develop a regioselective process which led to selective access to symmetrical 1,3,5- and unsymmetrical 1,2,4-trisubstituted aromatic compounds.³ Since then, the reaction has been extensively studied and a range of transition metal catalysts, mainly based on group 8-10 elements such as Ni, Co, Pd, Rh, Ru, and Ir, have been developed.⁴⁻²⁸ Moreover, after the pioneering work of Mori²⁹ and Starý³⁰ who used respectively chiral nickel and cobalt complexes in this reaction, significant progress has been made in asymmetric transition metal-catalyzed [2+2+2] cycloaddition reactions over the past decades.³¹⁻³⁸ This highly atom-economical transformation allows the formation of three new bonds in a single step and proceeds through either intermolecular, partially intramolecular or totally intramolecular processes to furnish a variety of (poly)cyclic skeletons with the latter strategy allowing for an excellent control of the pair- and regioselectivity (Figure 1).

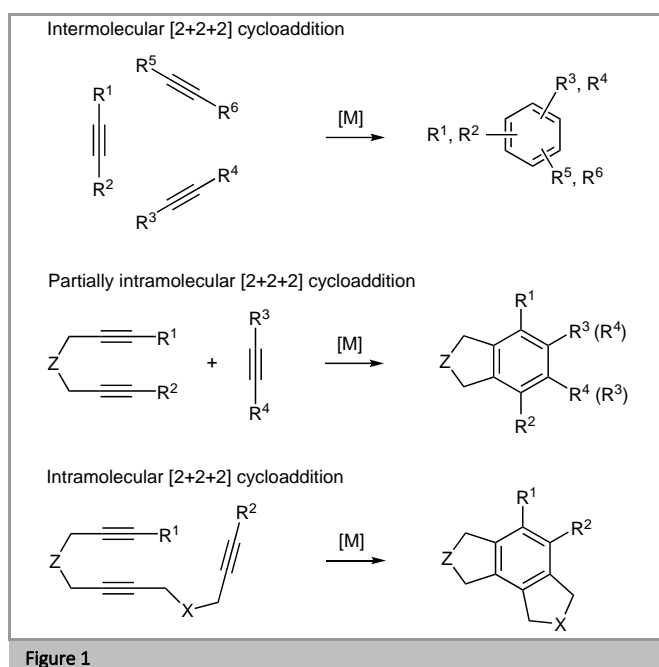


Figure 1

The general accepted mechanism for the transition metal-catalyzed alkyne cyclotrimerization involves the initial formation of a metallacyclopentadiene **B** or a metallacyclopentatriene **B'** complex after coordination of the metal to two alkyne ligands and oxidative coupling (Figure 2). Coordination of a third alkyne motif to this complex followed by alkyne insertion can then produce either a metallacycloheptatriene **D** or metallacycloheptatetraene **D'**, or a 7-metallanorbornadiene complex **E** resulting from a Diels-Alder cycloaddition, or a metallabicyclo[3.2.0]-heptatriene **F** formed through a [2+2] cycloaddition. Subsequent reductive elimination then affords the benzene product **G** while regenerating the metal catalyst.

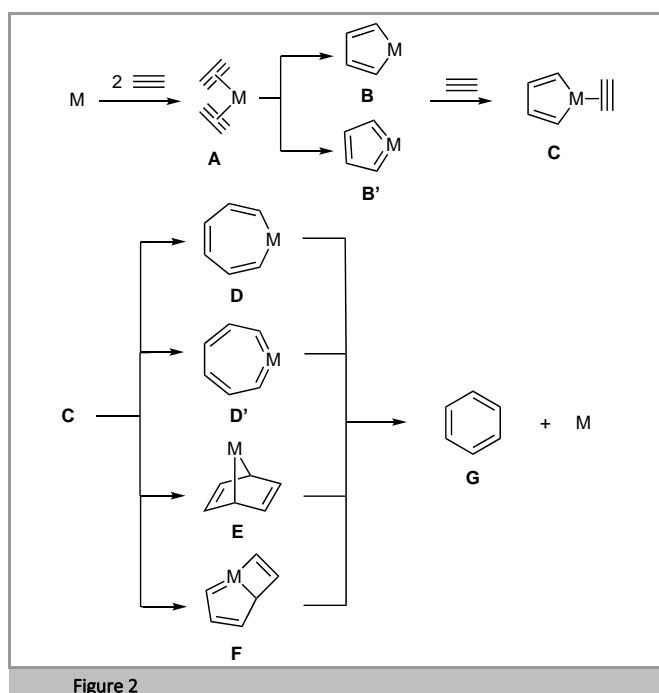
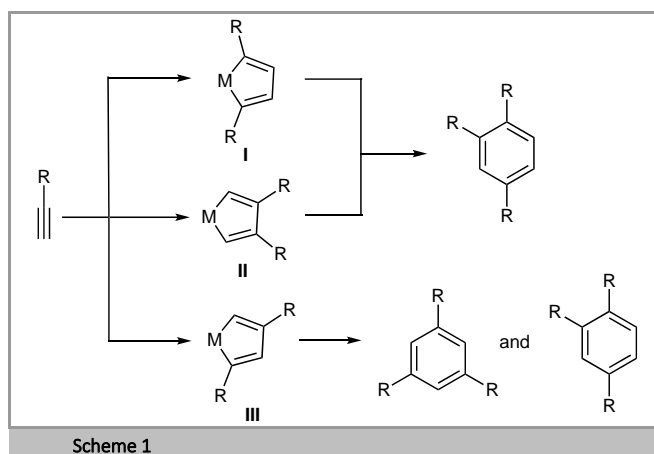


Figure 2

Scheme 1 shows the rationalization of the regioselectivity for the [2+2+2] cyclotrimerization of alkynes. The symmetrical

1,3,5-trisubstituted aromatic is usually the minor product although it is the less sterically hindered. The origin of the preferred regioselectivity can be explained by analysis of the potential metallacycle intermediates. The cyclotrimerization can proceed via three distinct metallacycles, which all favor the formation of the unsymmetrical product. However, only one of these intermediates (**III**) gives access to the symmetrical product.



Scheme 1

Unsaturated motifs such as alkenes, allenes, nitriles, cyanamides, isocyanates, imines, or carbonyl groups are suitable for this transformation, enabling a practical access not only to carbocycles but also to a range of heterocycles such as pyridines, pyridones, thiopyridones, or pyrones.³⁹⁻⁴⁷

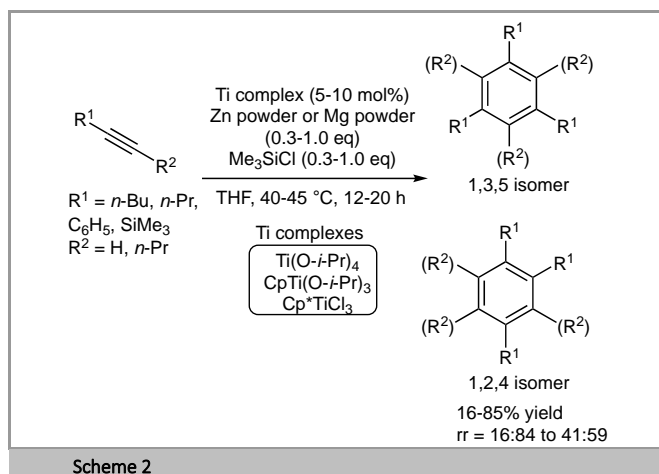
Some recent excellent reviews covering various aspects of the [2+2+2] cyclotrimerization reactions, including stereo-, chemo- and enantioselectivity as well as mechanistic aspects, have been published.⁴⁸⁻⁶¹ The aim of this non-exhaustive review is to summarize recent advances in the field of metal-catalyzed [2+2+2] cycloaddition from 2017 to July 2021. Metal-free [2+2+2] cycloaddition reactions will not be covered here.

2. Formation of Carbocycles

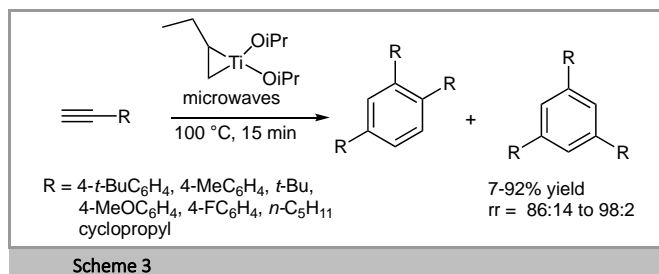
2.1. Intermolecular Reactions

2.1.1. Cyclotrimerization of Alkynes

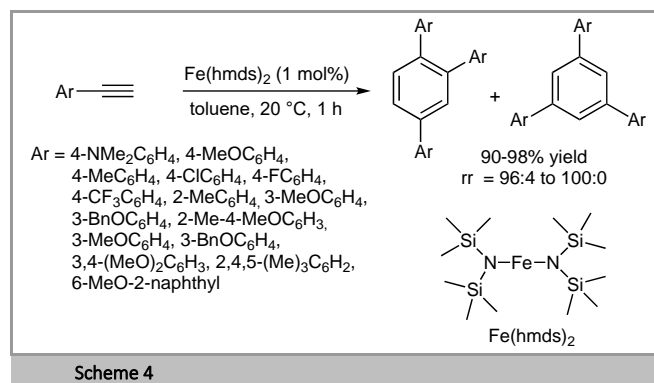
In 2017, Okamoto and co-workers demonstrated that low-valent titanium species catalyzed the [2+2+2] cycloadditions of alkynes using $\text{CpTi}(\text{O-}i\text{-Pr})_3$, CpTiCl_3 , or $\text{Ti}(\text{O-}i\text{-Pr})_4$ combined with Mg or Zn powder as metal reductant in the presence of Me_3SiCl that played a crucial role for the cycloaddition to proceed. Inter-, partially intra- and intramolecular alkyne cyclotrimerization can be accomplished in THF (0.5 M) at 40-45 °C for 12-20 h. Under these optimized reaction conditions, the corresponding 1,3,5- and 1,2,4-trisubstituted benzenes were obtained as a mixture of regioisomers (up to 41:59) in 16% to 85% yield (Scheme 2).⁶²



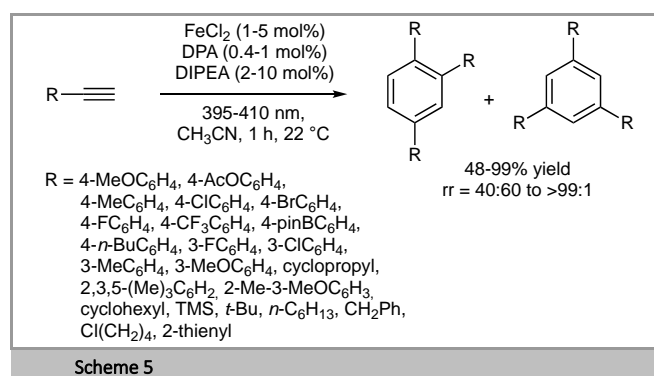
In 2019, Six and co-workers developed a convenient cyclotrimerization of alkynes using the low-cost $\text{Ti}(\text{O}-i\text{-Pr})_4/n\text{-BuLi}$ system to generate the active species titanacyclopropane (Scheme 3). The titanium-promoted cyclotrimerization process of terminal alkynes required 0.6 eq of $\text{Ti}(\text{O}-i\text{-Pr})_4$ and 0.9 eq of $n\text{-BuLi}$ with respect to the alkyne derivatives under microwave irradiation at 100 °C for 15 min to produce the 1,2,4 adducts with yields ranging from 7% to 92% and regioisomeric ratios (rr) up to >98:2. The titanium-mediated cyclotrimerization of disubstituted alkynes was also briefly studied. This practical protocol allowed a significant improvement compared to the previous developed reaction conditions (2.2 eq $\text{Ti}(\text{O}-i\text{-Pr})_4$ and 3.3 eq of $n\text{-BuLi}$ at room temperature).⁶³



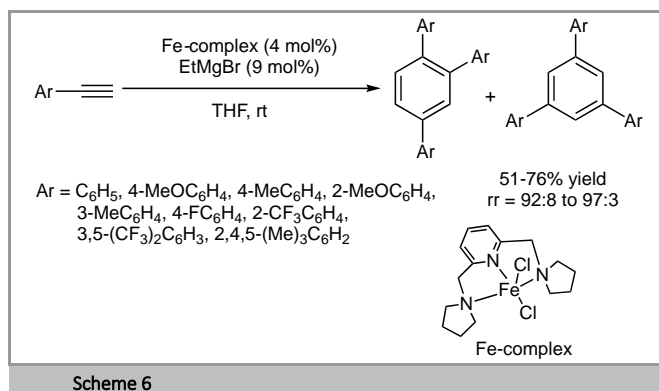
In 2017, Jacobi von Wangelin and co-workers succeeded in developing an iron-catalyzed cyclotrimerization of terminal alkynes using 1 mol% of $\text{Fe}(\text{hmds})_2$ in toluene at 20 °C for 1 h. No reducing reagent was required for such unprecedented transformation involving an Fe^{II} catalyst although $\text{Fe}(\text{OTf})_2$, FeCl_2 , $\text{FeCl}_2(\text{THF})_{1.5}$, $\text{Fe}(\text{OAc})_2$ were not effective for the reaction. Under optimized conditions, terminal alkynes underwent highly efficient cyclotrimerization delivering the corresponding 1,2,4-trisubstituted arenes with excellent level of regioselectivities and isolated yields. Aryl substituted alkynes bearing isoprenyl, *tert*-butyl, carboxymethyl and deuterium were also tolerated (not shown). Of note, extremely high turnover frequency (TOF) up to 180000 h^{-1} was achieved for the cyclotrimerization of a 1M solution of phenylacetylene within <1 min at 20 °C using 1 mol% of $\text{Fe}(\text{hmds})_2$. Unfortunately, cyclotrimerization of internal alkynes did not proceed under the standard conditions. Alternatively, the mixture of inexpensive $\text{FeCl}_2/\text{LiHMDS}$ can also be used for the cyclotrimerization (Scheme 4).⁶⁴



In 2020, Jacobi von Wangelin, Chakraborty and co-workers reported a photo-organo-iron cyclotrimerization of alkynes demonstrating the first dual catalytic protocol combining organic photoredox catalysis and iron-catalysis for synthetic applications (Scheme 5).⁶⁵ A photostable organic dye 9,10-diphenylanthracene (DPA) allowed the photo-catalytic reduction of FeCl_2 under visible light irradiation. The reaction proceeded under mild conditions (Vis light, 22 °C, 1 h) in 48%-99% yield with regiocontrol up to >99:1 to produce a broad array of trisubstituted arenes when using 1-5 mol% of the three inexpensive catalysts (dye, amine and FeCl_2) for this efficient transformation. Mechanistic studies were also performed.

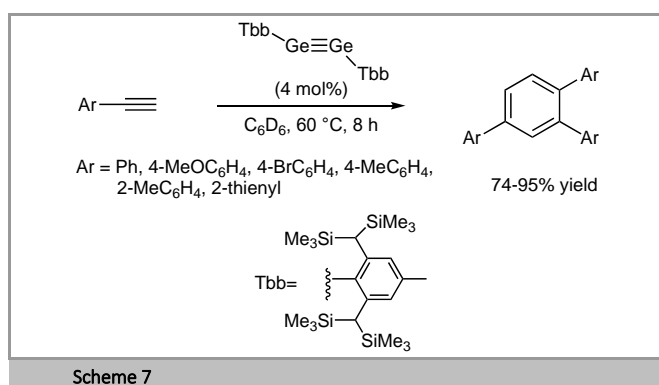


In 2019, Gunanathan and co-workers accomplished the regioselective [2+2+2] cyclotrimerization of terminal aryl and alkyl alkynes at room temperature upon activation of Fe -catalyst by a Grignard reagent to access 1,2,4-trisubstituted benzene derivatives by using simple well defined and easy accessible di(aminomethyl)pyridine ligated iron-pincer complexes (Scheme 6).⁶⁶ Terminal aryl alkynes were cyclized to provide the corresponding 1,2,4-trisubstituted isomers in 51-76% yield and up to 97:3 regioselectivities while aliphatic terminal alkynes led to 36-80% yield with poor regioselectivities. Hexa-substituted benzenes were obtained regioselectively as well through cyclotrimerization of the corresponding aryl alkyl internal alkynes although increasing the steric bulk on pincer Fe ligands decreased the regioselectivity for the cycloaddition reaction. A catalytic cycle for the Fe -catalyzed [2+2+2] cycloaddition reaction was proposed and mechanistic studies were investigated.



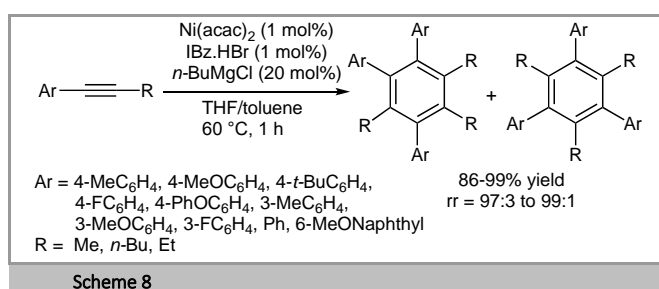
Scheme 6

In 2018, Sasamori and co-workers explored the scope of regioselective germanium-catalyzed cyclotrimerization of terminal arylacetylenes at 60 °C for 8 h in C₆D₆ using 4 mol% of an isolable digermine pre-catalyst TbbGeGeTbb, enabling the formation of C-C bonds in the absence of a transition-metal catalyst, to provide the corresponding 1,2,4-triarylbenzenes in 74-95% yield with complete regioselectivity and no 1,3,5-Ar₃C₆H₃ byproducts (Scheme 7).⁶⁷ Unfortunately, the reaction did not occur with internal alkynes. A reaction mechanism for the cyclotrimerization of terminal arylacetylenes was proposed.



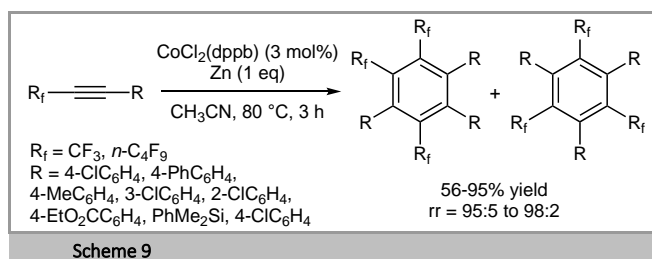
Scheme 7

In 2017, Hor, Zhao and co-workers described a catalytic [2+2+2] cyclotrimerization of unactivated internal alkynes by using a catalyst system combining Ni(acac)₂, IBz.HBr or IMES-HCl (1 mol%) as an imidazolium salt and *n*-BuMgCl (Scheme 8).⁶⁸ Unactivated alkyl(aryl)acetylenes and diarylacetylenes bearing either electron-donating or withdrawing substituents on the aryl ring were tolerated for this transformation although no reaction was observed with dialkylalkynes. The reaction proceeded at room temperature or 60 °C for 20 min or 1 h offering a practical synthetic route to access polysubstituted benzenes in 86-99% yield with regioselectivities up to 99:1.



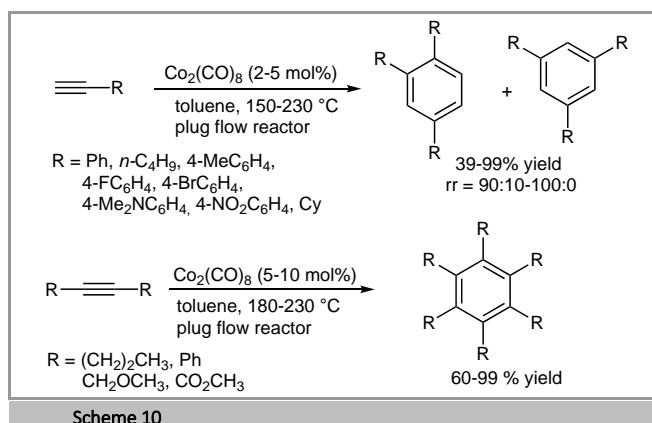
Scheme 8

In 2018, Konno and co-workers realized the cobalt-catalyzed [2+2+2] cycloaddition of an array of fluorine-containing alkynes using 3 mol% of CoCl₂(dppb) in CH₃CN at 80 °C for 3 h delivering the corresponding benzene derivatives in 56-95% yield with regioselectivities up to 98:2 (Scheme 9).⁶⁹ Additionally, intermolecular [2+2+2] cycloaddition of fluorinated alkynes with non-fluorinated diynes proceeded in the presence of 3 mol% of CoCl₂/(*S*)-BINAP, Zn metal and ZnI₂ to afford the desired fluorinated cycloadducts in 46-83% yield (not shown).



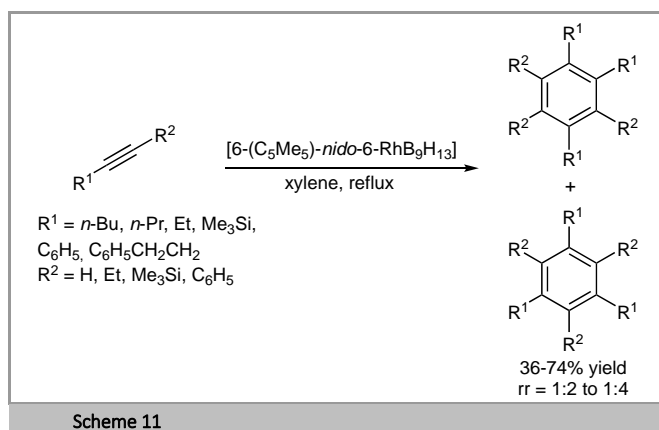
Scheme 9

In 2018, Pérez-Castells, Blanco-Urgoiti and co-workers reported cobalt-catalyzed scalable terminal and internal alkyne cyclotrimerizations and [2+2+2] cycloadditions of diynes and alkynes as well in a plug flow reactor (PFR) using 5-10 mol% of the inexpensive cobalt catalyst Co₂(CO)₈ (Scheme 10).⁷⁰ The reactions showed a broad scope and was an interesting alternative for scale-up applications. Cyclotrimerization of seven terminal alkynes was carried out in PFR in toluene in 3.5-60 min reaction time and 150-230 °C to provide the cyclized products in 83-99% yield with up to 99:1 regioselectivity. The procedure was scaled-up with 10 g of phenylacetylene using a total reaction time of 105 min at 180 °C in the presence of 2 mol% of Co₂(CO)₈ to give the corresponding 1,2,4 isomer in 92% yield and 99:1 regioselectivity. The kinetics and the selectivities of the reaction were probably influenced by the intensification conditions used in microreactors. The highly regioselective cyclotrimerization of internal alkynes was also studied in the presence of 5-10 mol% of Co₂(CO)₈ to give the hexasubstituted products in 60-99% yield. Finally, [2+2+2] cycloaddition of α,ω-diynes and alkynes was achieved using Mo(CO)₆, Co₄(CO)₁₂, Rh₂(CO)₄Cl₂, Ru₃(CO)₁₂, CpCo(CO)₂, Cr(CO)₆, and Co₂(CO)₈ with variable yields ranging from 21 to 85% by utilizing a careful selection of reaction conditions (alkyne equivalents, temperature, and residence time) to favor the cycloaddition.

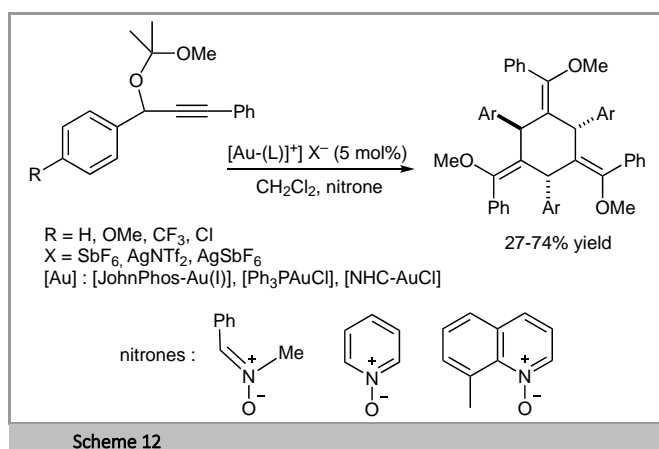


Scheme 10

In 2018, Spencer and co-workers disclosed the cyclotrimerization of a range of internal and terminal alkynes catalyzed by rhodadecaborane [6-(C₅Me₅)-nido-6-RhB₉H₁₃] in xylene for 2 h yielding a mixture of 1,3,5- and 1,2,4-trisubstituted benzene derivatives in 36-74% yield with 1:2-1:4 ratio respectively (Scheme 11).⁷¹ These results showed that large-vertex metallaborane can be a useful catalyst for [2+2+2] cycloaddition of alkynes.

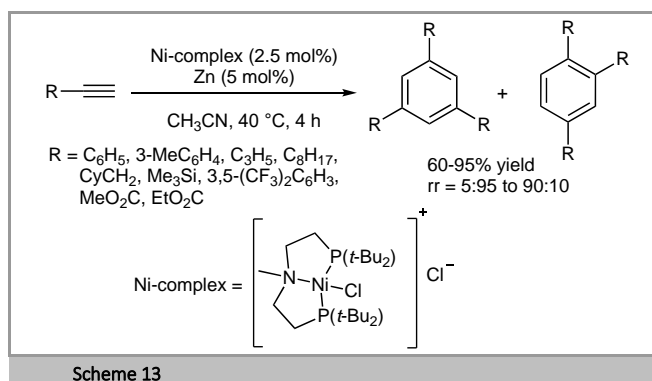


In 2017, Fiksdahl and co-workers published the regio- and chemoselective Au(I)-nitron-catalyzed [2+2+2] cyclotrimerization of 1,3-diarylpropargyl acetals (Scheme 12).⁷² This intermolecular regioselective [2+2+2] cyclotrimerization of propargyl substrates led to highly functionalized cyclohexylidene products in 27-74% yield. The cyclotrimerization is suggested to proceed through allenic intermediates via gold-catalyzed 1,3-alkoxy rearrangement. The authors demonstrated that catalytic amounts of nitron were crucial to achieve selective cyclotrimerization. In this context, the crystalline phosphane-Au(I)-nitron complex showed comparable catalytic performance compared to Au(I)-nitron complex prepared in situ. X-ray analysis of the Au(I)-nitron catalyst confirmed the linear nitron-O-Au(I)-P coordination mode of the catalyst.

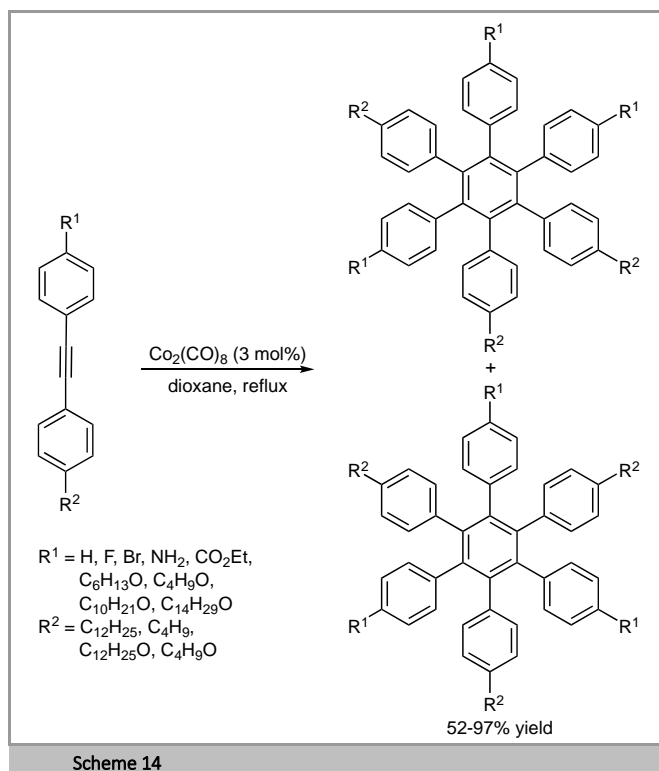


In 2017, Sivasankar and co-workers accomplished the [2+2+2] Ni(II)-catalyzed cycloaddition of alkynes in the presence of 5 mol% of zinc at 40 °C for 4 h using 2.5 mol% of [(PNP)NiCl]Cl complexes (Scheme 13).⁷³ Optimization of the reaction conditions showed that the use of Zn in CH₃CN as a

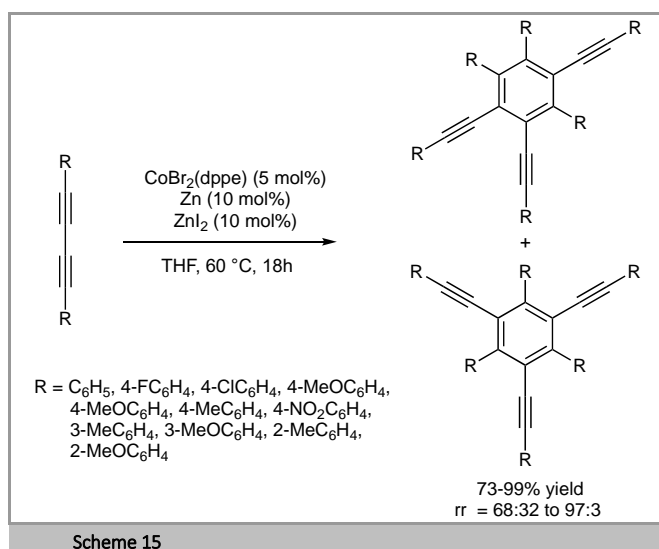
reductant, which allowed the reduction of Ni(II) to Ni(0), gave better results compared to Sn and Mg. The solvent also influenced the selectivity: dichloromethane and THF afforded the dimerized product as a major product in low yields. Finally, the electronic nature of the alkynes played a role in controlling the selectivity: electron-rich alkynes such as alkyl-substituted alkynes led to the 1,3,5-substituted benzene derivatives as the major products in 70-86% yield with a regioisomeric ratio of 75:25 to 90:10 while the electron-deficient alkynes furnished the 1,2,4-substituted benzene derivatives as the major products in 65-95% yield with a regioisomeric ratio of 5:95.



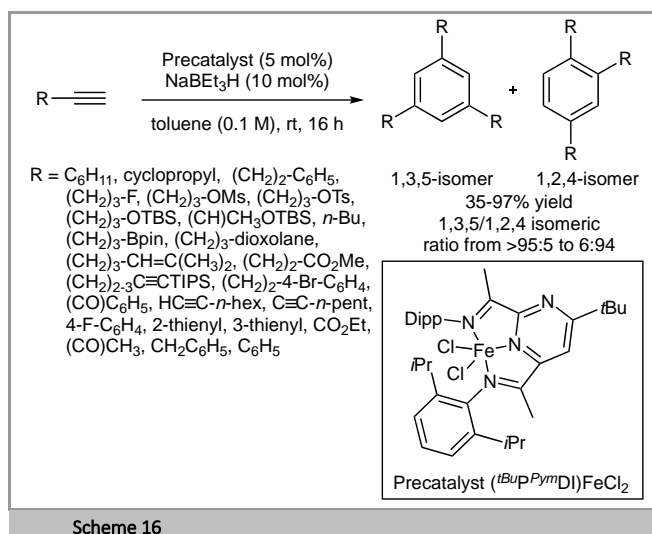
In 2017, Chen and co-workers studied the operationally simple cobalt-catalyzed cyclotrimerization of a series of unsymmetrical diarylalkynes using Co₂(CO)₈ as catalyst to access 1,2,4-regioisomer and 1,3,5-regioisomer in 52-97% yield with specific regioselectivity by choosing the appropriate electron withdrawing groups (EWGs) and donating groups (EDGs) on the aryl ring of the alkyne (Scheme 14).⁷⁴ The role of some electron EWGs and EDGs in diaryl-substituted alkynes was investigated to access the desired regioisomer allowing to control the chemo- and regioselectivity of the cyclotrimerization of unsymmetrical diarylalkynes. Indeed, the authors established a selection of substituents in diaryl-substituted alkynes for the preparation of 1,2,4-regioisomer and 1,3,5-regioisomer. When both side of the diarylalkyne were substituted with various alkoxy groups, exclusive formation of 1,3,5-regioisomer was observed in 64-91% whereas the appropriate electron-deficient substituent at the aryl ring promoted the formation of 1,2,4-regioisomer in 20-72% yield.



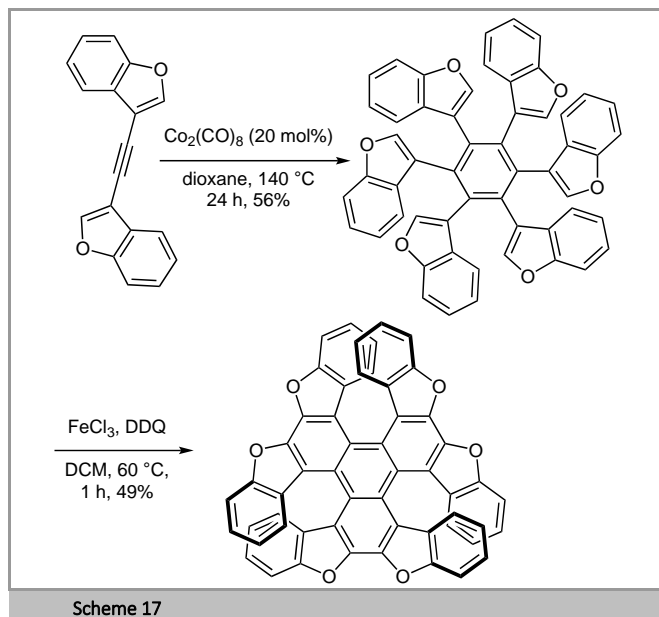
In 2019, Hilt and co-worker investigated a chemoselective cobalt(I)-catalyzed [2+2+2] cyclotrimerization of symmetrical and unsymmetrical 1,4-disubstituted 1,3-butadiynes. The reaction was achieved in the presence of 5 mol% of $\text{CoBr}_2(\text{dppe})$ with 10 mol% of Zn and 10 mol% of ZnI_2 in THF at 60 °C for 18 h (Scheme 15).⁷⁵ With respect to unsymmetrical 1,3-butadiynes, a single 1,2,4-substituted isomer was obtained in 15-97% yield and >99:1 regioselectivities (not shown). Nevertheless, a steric effect of the alkyne residue was observed toward the chemo- and regioselectivity of the cycloisomerization ($\text{R}^2 = 4\text{-F-C}_6\text{H}_4$, $\text{R}^1 = t\text{-Bu}$, >99:1 rr, $\text{R}^1 = \text{Et, } i\text{-Pr}$, 7 detectable isomers). When symmetrical aryl-substituted 1,3-butadiynes bearing electron-donating or -withdrawing groups on the aryl ring were cyclotrimerized, 73-99% yields were obtained with regioselectivities varying from 68:32 to >99:1 rr (not shown). A broad range of 1,2,4 regioisomers were prepared.



In 2021, Roşca and co-workers developed the first iron-based catalytic intermolecular cyclotrimerization of terminal aliphatic alkynes in 35-97% yield. In the presence of 5 mol % of precatalyst $(t\text{BuPPymDI})\text{FeCl}_2$ and 10 mol % of NaBEt_3H in toluene at room temperature, 1,3,5-substituted arenes were regioselectively produced with 1,3,5/1,2,4 ratios up to >95:5 (Scheme 16). Preliminary mechanistic investigations suggested that the enhanced π -acidity of the pyrimidine ring, combined with the hemilability of the imine groups coordinated to the iron center, facilitated this transformation. It is noteworthy that the precatalyst was sufficiently stable to allow weighing without exclusion of air/ moisture. Although the reaction tolerated a great variety of substituents on the alkyne, the regioselectivity decreased for alkynes with electron-withdrawing groups.⁷⁶

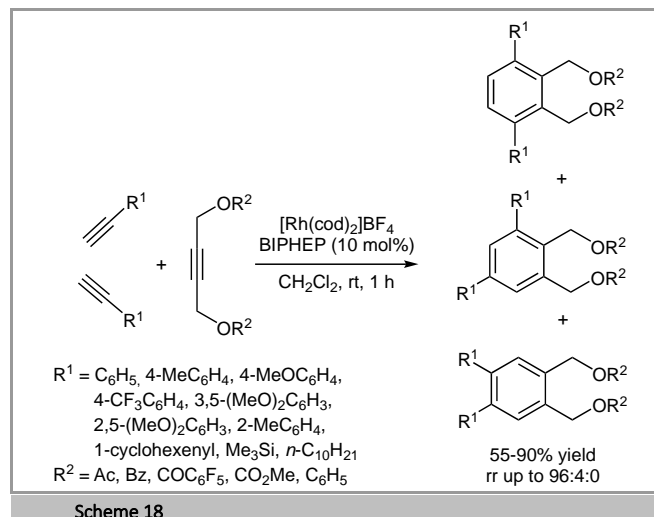


In 2021, Yang and co-workers reported a synthesis of a structurally unusual furan-based triple oxa[7]helicene involving a [2+2+2] cycloaddition. The cyclotrimerization of 1,2-di(benzofuran-3-yl)ethyne in the presence of 20 mol% of $\text{Co}_2(\text{CO})_8$ afforded the cycloadduct in 56% yield. This intermediate underwent an intramolecular dehydrogenative annulation to furnish the triple oxa[7]helicene in 49 % yield (Scheme 17).⁷⁷

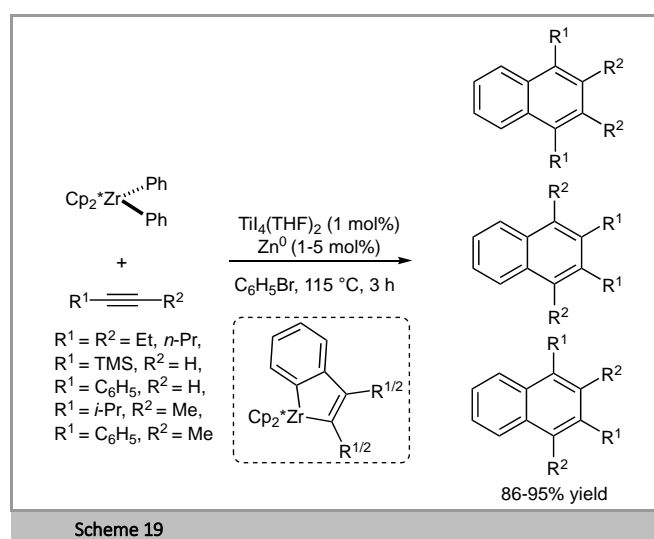


2.1.2. [2+2+2] Cycloaddition of Two Different Alkynes

In 2017, Tanaka and co-workers displayed that 10 mol % of BIPHEP Rh(I) complex enabled the chemo and regioselective intermolecular cross-cyclotrimerization of nonactivated terminal and internal alkynes at room temperature in CH_2Cl_2 for 1 h using arylacetylenes and 1,4-butanediol derivatives respectively to access (3,6-diaryl-1,2-phenylene)-dimethanol derivatives in 55-90% yield with up to 96:4:0 rr (Scheme 18).⁷⁸ Indeed, Biphep led to the slightly highest yield whereas MeO-Biphep, Difluorphos, Segphos, Binap, H₈-Binap were also tested with no significant difference on the chemo- and regioselectivities of the transformation. The substrate scope demonstrated that using sterically demanding 1,4-dibenzoyloxy-2-butyne instead of 1,4-diacetoxy-2-butyne increased the yield (84% vs 64%) and the regioselectivity as well (87:6:7 vs 82:7:11) whereas the use of electron-deficient penta-fluorophenyl derivative decreased the yield to 68% while maintaining similar regioselectivity (86:6:8). With respect to terminal alkynes, non-substituted phenylacetylene, *para*-substituted phenylacetylenes and 3,5-dimethoxyphenylacetylene furnished the corresponding cross-cyclotrimerized products in 68-90% yield with up to 89:7:4 regioselectivity. The authors clearly established that electronically biased combination of nonactivated and electron-deficient alkynes required for other transition-metal complexes, such as iridium, ruthenium, nickel, and palladium was not crucial to achieve good chemo- and regioselectivity in the cationic Rh(I)-catalyzed intermolecular cross-cyclotrimerization.

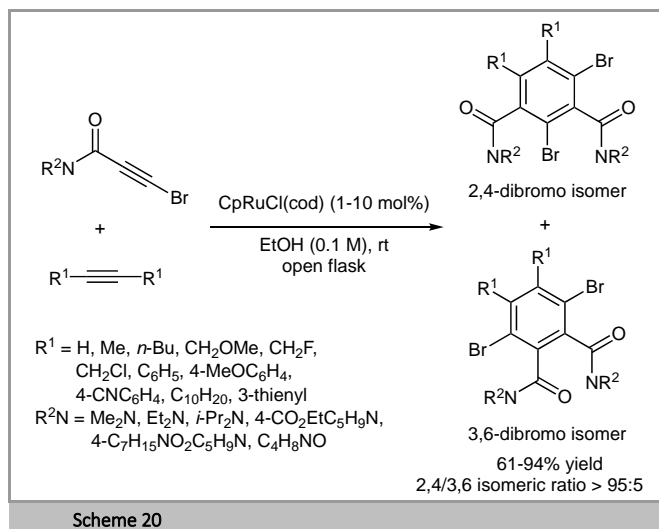


Because naphthalenes present broad applications in the photovoltaics, electronics and pharmaceutical industries, practical economical routes to prepare such compounds are highly desirable. In 2019, Tonks and co-workers described the Ti-catalyzed [2+2+2] cycloaddition of arynes and alkynes using Cp^*ZrPh_2 to access highly substituted naphthalene derivatives in 86-95% yield (Scheme 19).⁷⁹ The reaction was performed in the presence of 1 mol% of $\text{TiI}_4(\text{THF})_2$ with 1-5 mol% of Zn^0 in $\text{C}_6\text{H}_5\text{Br}$ at 115 °C for 3 h using Cp^*ZrPh_2 and the corresponding alkynes. The authors demonstrated that bulky Cp^* rings were essential to suppress the formation of parasitic metalloindane byproducts. Various potential alkyne coupling partners were tested showing that the formation of the desired naphthalene products was best correlated to alkyne steric rather than electronic properties. Considering the product selectivity toward naphthalenes over alternative possible coupling products including triphenylene or phenanthrene derivatives, a mechanism in which a titanacyclopentadiene was intercepted by a Zr-benzynes adduct was suggested.

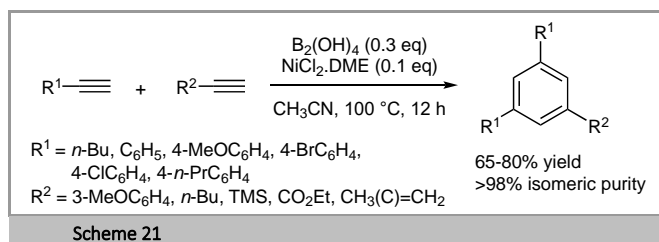


In 2020, Oakdale and co-worker developed a highly regio- and chemoselective intermolecular cyclotrimerization to access dihalogenated isophthalimides. Symmetrical internal alkynes and 3-halopropionamides led to the desired cycloadducts in the presence of 1-10 mol% of $\text{CpRuCl}(\text{cod})$ as a catalyst. When

ethanol was used instead of CH_2Cl_2 as a solvent, the regioselectivity of the reaction was improved to >95:5. Despite the high amount of catalyst required for some substrates (up to 10 mol %), the reaction occurred at room temperature with no need of inert atmosphere in 61-94% yield. The authors demonstrated the robustness of the reaction and its versatility by establishing a novel synthetic way to phthalimide pharmacophores (Scheme 20).⁸⁰

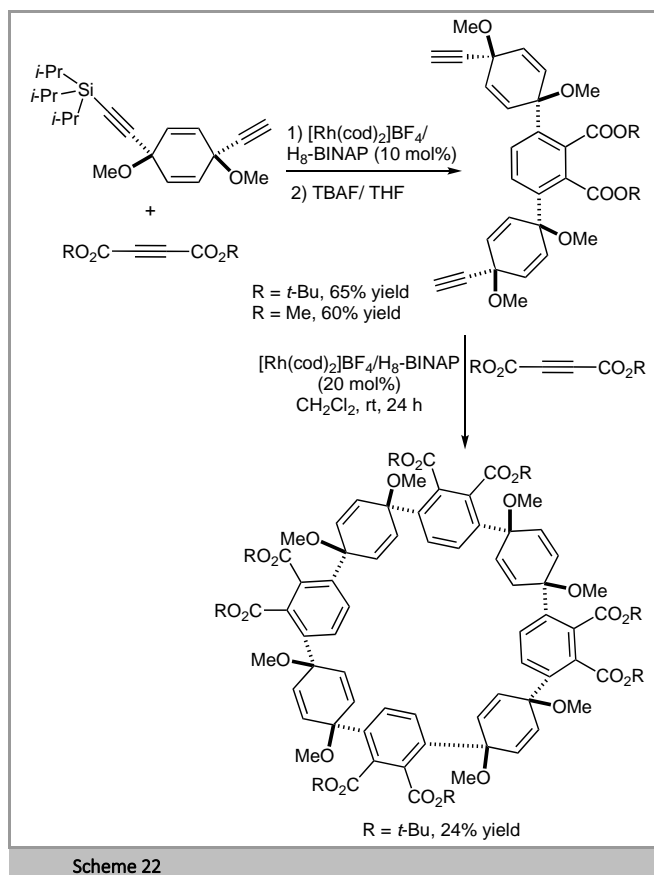


In 2021, Wang and co-workers reported a regioselective tetrahydroxydiboron and nickel-catalyzed cyclotrimerization occurring in acetonitrile at 100 °C giving 1,3,5-trisubstituted benzenes in 65-80% yield and isomeric purity above 98%. The $\text{Ni-B}(\text{OH})_2$ catalyst was generated *in situ* by transmetalation in the presence of 10 mol% of $\text{NiCl}_2\cdot\text{DME}$ and 30 mol% of $\text{B}_2(\text{OH})_4$. To explain the high regioselectivity of this reaction, the authors proposed a mechanism involving nickel-boronic acid derivative interaction and hydrogen bonding between the terminal alkyne and the hydroxyl groups on the boron. The 1,3,5-regioselectivity was observed either with one or with two different terminal alkynes (Scheme 21).⁸¹



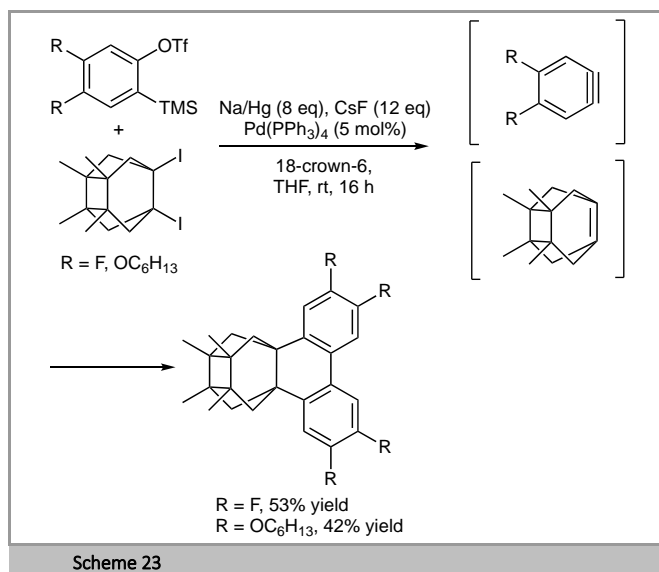
In 2017, Tanaka and co-workers disclosed the synthesis of C4- and C2-symmetrical [8]CPP-octacarboxylates via macrocyclization through Rh-catalyzed intermolecular stepwise cross-cyclotrimerizations and subsequent reductive aromatization (not shown) (Scheme 22).⁸² The first intermolecular cross-cyclotrimerization of diyne ($\text{R} = \text{Me, } t\text{-Bu}$) in which one terminal position is protected with the triisopropylsilyl group, and di-*tert*-butyl acetylenedicarboxylate was performed in the presence of 10 mol% of cationic $\text{Rh}(\text{I})/\text{H}_8\text{-BINAP}$ catalyst at room temperature in CH_2Cl_2 for 16 h to give the protected diyne that was deprotected with TBAF to access the terminal diyne ($\text{R} = \text{Me, } t\text{-Bu}$ 60% and 65% yields,

respectively). The second intermolecular cross-cyclotrimerization of the terminal diyne proceeded by using 20 mol% of $\text{Rh}(\text{I})/\text{H}_8\text{-BINAP}$ at room temperature in CH_2Cl_2 for 24 h to provide [8]CPP precursor in 24% yield.

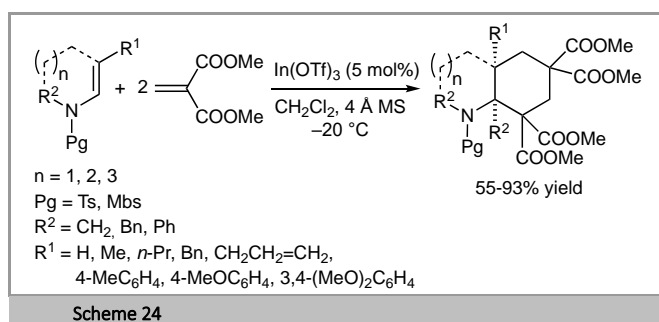


2.1.3. [2+2+2] Cycloaddition of Alkynes/Alkenes with Alkenes/Enamides

In 2018, Peña and co-workers reported the Pd-catalyzed [2+2+2] cocycloaddition of arynes with pyramidalized non conventional alkene derivatives (Scheme 23).⁸³ Different conditions and metal complexes such as $\text{Pd}_2(\text{dba})_3$, $\text{Pt}(\text{PPh}_3)_4$, AuClPPh_3 , $\text{Ni}(\text{PPh}_3)_4$ and $\text{Pd}(\text{PPh}_3)_4$ have been tested for the reaction. The cyclotrimerization reactions have been realized using 5 mol% of $\text{Pd}(\text{PPh}_3)_4$ and Na/Hg combined with CsF in THF at room temperature for 16 h yielding the corresponding adducts in 15-53% yield with several substituted aryne precursors. In this context, five different substituted or polycyclic arynes successfully reacted with the pyramidalized alkene via Pd-catalysis demonstrating the generality of the reaction.

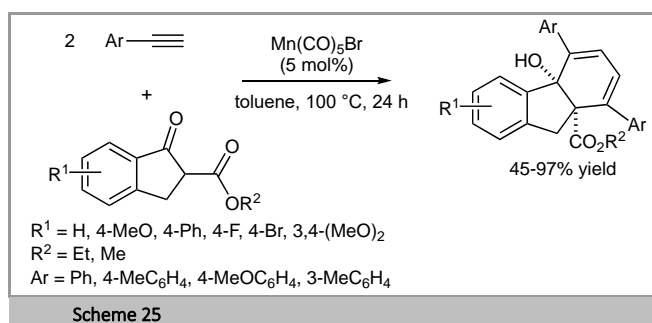


In 2019, Tang, Wang and co-workers examined [2+2+2] cycloaddition reactions of *N*-sulfonyl enamides and dimethyl methylenemalonate (Scheme 24).⁸⁴ Under the optimal conditions, the reaction proceeded smoothly at $-20\text{ }^{\circ}\text{C}$ in CH_2Cl_2 using 5 mol% of $\text{In}(\text{OTf})_3$ in the presence of 4 Å MS to provide the cyclohexane derivatives in 55-93% yield. No improvement of the cyclization was observed either when using copper salts such as $\text{Cu}(\text{NTf}_2)_2$, $\text{Cu}(\text{ClO}_4)_2 \cdot 6\text{H}_2\text{O}$ or metal chloride (FeCl_3 and InCl_3) while $\text{Ni}(\text{OTf})_3$ and $\text{Yb}(\text{OTf})_3$ were inactive. A lower yield was obtained with $\text{Fe}(\text{OTf})_3$. Finally, the reaction catalyzed by $\text{In}(\text{OTf})_3$ was completed in a shorter time and led to the best results. Different *N*-protecting groups such as electron-withdrawing *p*-fluorotosyl (F_Ts), *p*-methoxy benzene sulfonyl (Mbs) and tosyl (Ts) groups were tested for the cycloaddition. *N*-Ts 2,3-dihydropyrroles bearing 4-alkyl substituents (Me, *n*-Pr, Bn, allyl, and propargyl) were efficiently cyclized to the corresponding octahydroindole derivatives in 80%-93% yield in 12 h whereas *N*-Mbs 4-aryl 2,3-dihydropyrroles produced the arylated octahydroindoles in 55-61% yield with a longer reaction time of 60 h (not shown).



In 2019, Maji and co-workers displayed the Mn-catalyzed [2+2+2] cycloaddition of various β -ketoesters with readily available unactivated terminal alkynes via domino-Markovnikov anti-Markovnikov fashion, in the presence of 5 mol % of $\text{Mn}(\text{CO})_5\text{Br}$ at $100\text{ }^{\circ}\text{C}$ in toluene for 24 h to access a tricyclic framework as a single diastereoisomer (Scheme 25).⁸⁵ This atom-economical and environmentally sound method enabled an efficient approach for the construction of all-carbon quaternary centers and polycyclic hydrocarbon scaffolds

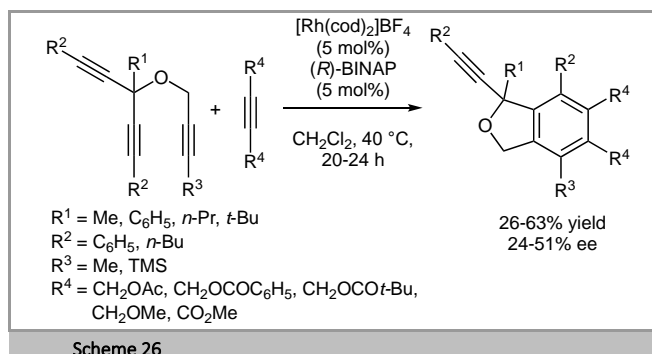
allowing the formation of new C-C single bonds in a regio- and stereoselective manner. The electronic influence of the arene substituents (MeO, Ph, F, Br) of the β -ketoesters had no significant influence on the domino reaction and the cycloadducts were prepared as single regio- and diastereoisomers in 70-80% yield. However, the reaction of dimethoxysubstituted β -ketoester with phenylacetylene yielded the tricyclic carbocycle in 45% yield. Additionally, other substituted aryl acetylenes were good coupling partners to access the carbocycles in 56-78% yield. Unfortunately, the alkyl alkynes remained unreacted under the optimized reaction conditions. Experiments involving deuterium labeling, kinetic, catalytic, and stoichiometric reactions with plausible intermediates were conducted to elucidate the reaction mechanism.



2.2. Partially Intramolecular [2+2+2] Cycloaddition Reactions

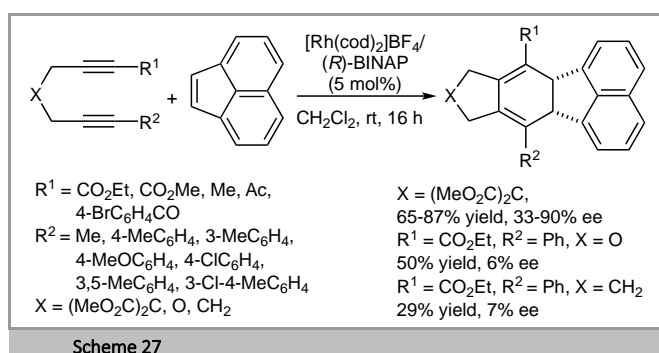
2.2.1. Rhodium-Catalyzed [2+2+2] Cycloaddition

In 2018, our group developed the cationic Rh/Binap [2+2+2] cycloaddition of diversely substituted triynes with internal functionalized alkynes. The optimization of the conditions enabled to access 1,1-disubstituted 1,3-dihydrobenzo[*c*]furans containing quaternary carbon stereogenic centers in yields up to 63% and moderate 24-51% ee (Scheme 26).⁸⁶ A plausible reaction mechanism for the formation of chiral 1,3-dihydrobenzo[*c*]furans was proposed involving two different pathways.

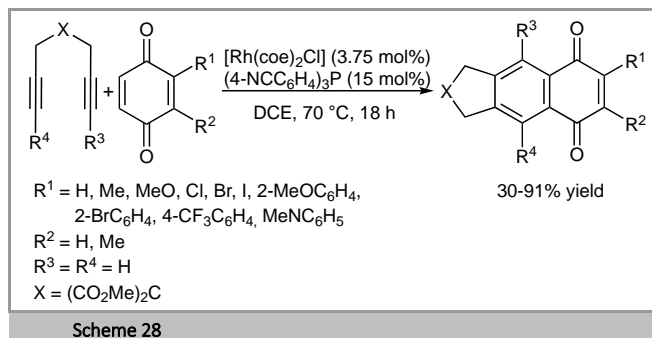


In 2018, Tanaka and co-workers established that 5 mol% of cationic Rh-(I)/(*R*)-Binap complex catalyzed the [2+2+2] cycloaddition of unsymmetrical α,ω -diynes with acenaphthylene at room temperature in CH_2Cl_2 for 16 h leading to pentacyclic 1,3-cyclohexadienes in up to 92% yield with up to 92% ee (not shown) values (Scheme 27).⁸⁷ It should be noted that

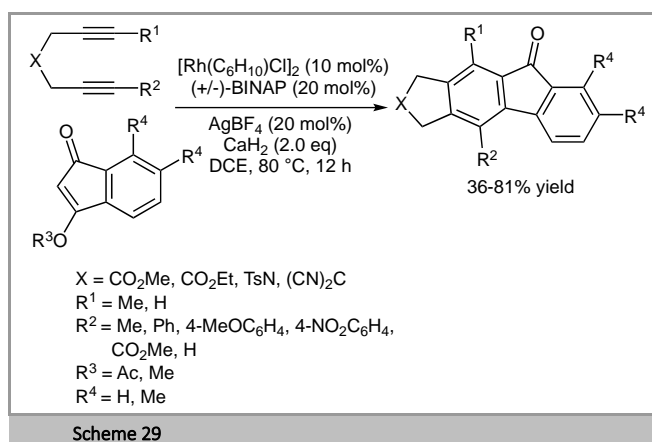
enantioselectivity highly depended on the structures of the α,ω -diynes involved in the cyclization. Interestingly, the structural features of α,ω -diynes to reach high enantioselectivity were opposite to those previously developed by the authors in cationic rhodium(I)-catalyzed asymmetric [2+2+2] cycloaddition of α,ω -diynes with indene, using the (*R*)-Difluorophos ligand developed in our group.⁸⁸ A possible mechanism for Rh-catalyzed asymmetric [2+2+2] cycloaddition of α,ω -diynes with acenaphthylene was proposed. The authors invoked several possible hapticities (η^2 , η^3 , and η^5 modes) in the coordination of acenaphthylene to the cationic Rh that might possibly affect stereoselectivities of the enantiodetermining steps. It should be mentioned that non asymmetric version of the [2+2+2] cycloaddition can be performed by using commercially available Biphep as a ligand with comparable yield to those observed with Binap.



In 2020, Bower, Junior and co-workers outlined a Rh-catalyzed [2+2+2] cycloaddition between 1,6-diynes and benzoquinones (Scheme 28).⁸⁹ Optimization of the reaction showed that $[\text{Cp}^*\text{Ru}(\text{MeCN})_3]\text{PF}_6/\text{Et}_4\text{NCl}$ and Rh-based catalytic systems such as $[\text{Rh}(\text{cod})_2]\text{OTf}$ or $[\text{Rh}(\text{cod})\text{Cl}]_2$ led to low yields, CoCl_2 and NiCl_2 being ineffective for the cyclization. Best results were achieved in the presence of $[\text{Rh}(\text{coe})\text{Cl}]_2$ combined with 4-(NCC_6H_4)₃P at 70 °C in dichloroethane for 18 h to access challenging naphthoquinones in up to 91% yield. In general, benzoquinones with electron-donating substituents were highly effective. The reaction accommodated halogen substituents on the benzoquinone unit. The protocol also tolerated naphthoquinones as a coupling partner. Alternatively, electron-deficient benzoquinones were not suitable substrates and led to decomposition products. Considering the 1,6-diynes: terminal 1,6-diynes with different linkers were effective partners as well as internal alkyl-substituted alkynes and aryl-substituted alkynes. More elaborate 1,6-diynes containing indole and furan-based systems can be employed as well. Finally, application to a short total synthesis of the lignan natural product justicidone demonstrated the utility of the method.

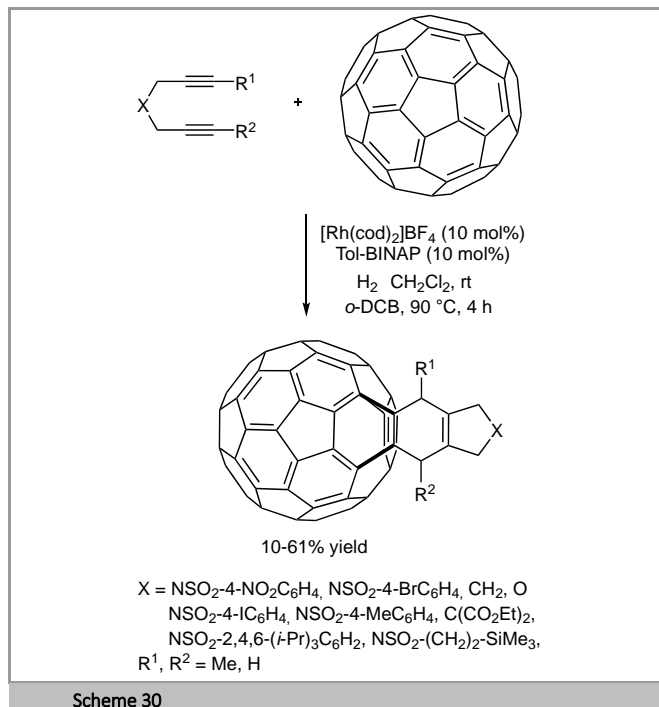


In 2020, Amatore and Commeiras reported Rh-catalyzed [2+2+2] cycloaddition reaction of α,ω -diynes with 3-acetoxy or 3-alkoxyindenediones as surrogates of the highly reactive benzocyclopentynone 2π partner, in the presence of 10 mol% of $[\text{Rh}(\text{C}_6\text{H}_{10})\text{Cl}]_2$ and racemic Binap combined with AgBF_4 with CaH_2 as an hydride source additive at 80 °C in anhydrous 1,2-dichloroethane for 12 h to provide the desired substituted fluorenones in 36-81% yield (Scheme 29).⁹⁰ Optimization of the reaction indicated that cycloaddition carried out in the presence of AgSbF_6 or AgOTf led to side reactions. Variable yields were obtained with diynes bearing different tethers (up to 81% with a gem-biscyano tether). Non-substituted diynes at the alkyne termini, diynes bearing different terminal groups such as phenyl and *p*-substituted phenyl with electron-donating and withdrawing substituents on the aryl ring led to a regioselectivity of 1:1, whereas diynes having at least one methylester group at the alkyne provided complete regioselectivity. However, the reaction of unsymmetrical diyne with indenone did not occur and gave a complex mixture. Finally, the method was also extended to the synthesis of an anthracene type derivative in 91% yield. This [2+2+2] cycloaddition offered a straightforward and tunable method to access challenging fluorenone-type derivatives.

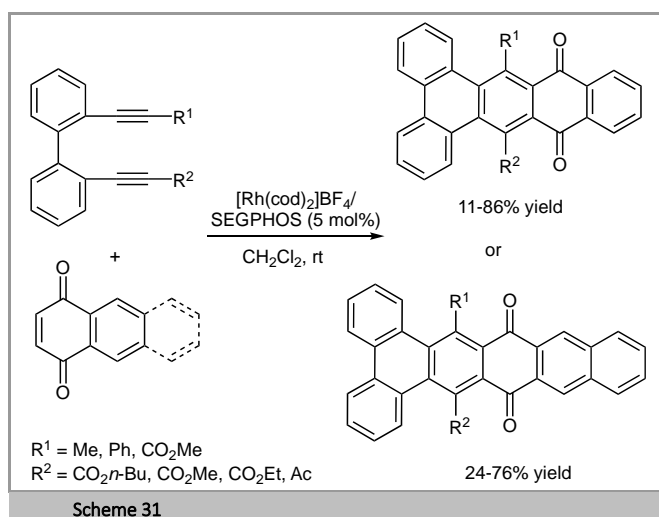


In 2018, Lledo, Roglans, Solà, and co-workers showed an expeditious preparation of open-cage fullerenes employing Rh(I)-catalyzed cycloaddition of diynes and C₆₀ to provide a cyclohexadiene-fused fullerene, which concomitantly underwent a formal [4+4] photocyclisation and retro-[2+2+2] rearrangement to access open-cage fullerenes. This modulate efficient cascade process was performed using 10 mol% of cationic $[\text{Rh}(\text{cod})_2]\text{BF}_4/\text{Tol-Binap}$ to produce the open-cage fullerene in 10-61% yield (Scheme 30).⁹¹ DFT calculations demonstrated that the transformation occurred

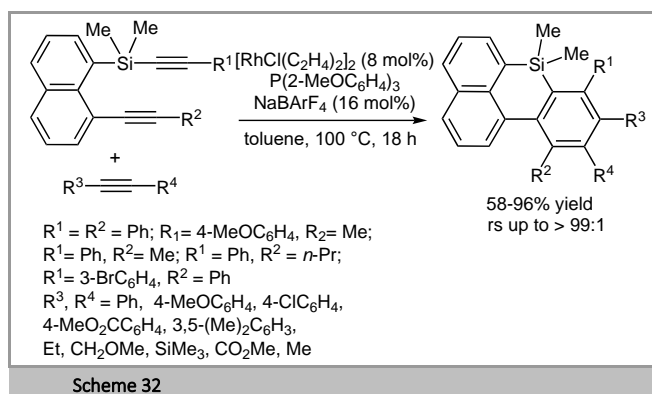
through a Rh-catalyzed [2+2+2] cycloaddition via a rhodabicyclo[3.2.0]heptadiene intermediate to provide a cyclohexadiene-fused C₆₀ intermediate. The initial oxidative coupling step of the rhodium-catalyzed [2+2+2] cycloaddition is the rate-determining step of the whole reaction pathway.



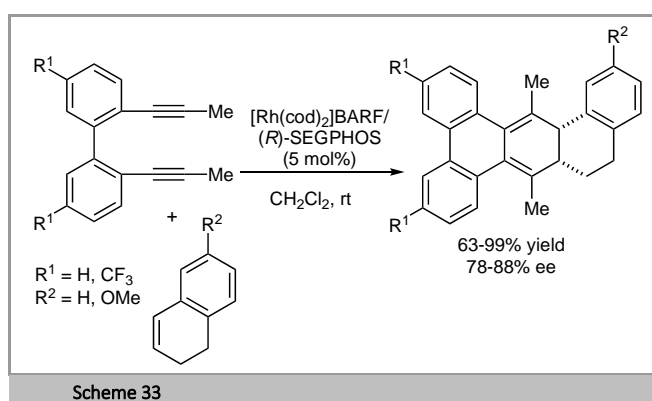
In 2019, Tanaka and co-workers succeeded in developing Rh(I)/Segphos [2+2+2] cycloaddition of biphenyl-linked 1,7-diynes with 1,4-naphthoquinone and anthracene-1,4-dione (Scheme 31).⁹² In the presence of 5-20 mol% of the Rh-complex, spontaneous aromatization occurred upon removal of the cationic Rh-complex as well as the desired [2+2+2] cycloaddition to provide dibenzotetracenediones (11-86% yield) and dibenzopentacenediones (24-76% yield), respectively. In addition to unsymmetrical diynes, symmetrical diynes reacted in 56% yield. Cycloaddition with malonate-linked 1,6 worked as well. Interestingly, dibenzotetracene showed blue fluorescence with a good quantum yield.



In 2020, Shintani and co-workers developed the synthesis of 7*H*-benzo[*e*]naphtho[1,8-*bc*]silines through Rh-catalyzed [2+2+2] cycloaddition of alkynyl(8-alkynyl-1-naphthyl)silanes with internal alkynes by using P(2-MeOC₆H₄)₃ as a ligand yielding a range of benzonaphthosilines in 58-96% yield and regioselectivity up to >99:1 (Scheme 32).⁹³ An asymmetric version of this process has been investigated using Rh/3'-methylated (*R*)-MeO-mop to provide silicon-stereogenic benzonaphthosilines in 62% yield with 80% ee.

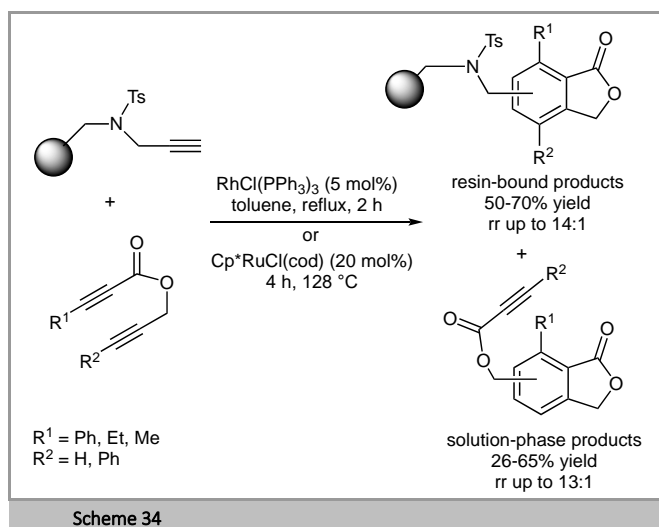


In 2020, Tanaka and co-workers displayed the successful enantioselective [2+2+2] cycloaddition of bi-phenyl linked internal 1,7-diyne (2,2'-di(prop-1-yn-1-yl)-5,5'-bis(trifluoromethyl)-1,1'-biphenyl) with 1,2-dihydronaphthalene (6-methoxy-1,2-dihydronaphthalene) followed by the diastereoselective Diels-Alder reaction and aromatization. The reaction proceeded using cationic Rh(I)/(*R*)-Segphos complex to access distorted π -extended chiral triptycenes, consisting of three distinct aromatic rings, in 63->99% yield and up to 88% ee values (Scheme 33).⁹⁴ In this approach, the use of the electron-deficient diyne and the electron-rich alkene was essential to suppress the undesired carbocation rearrangement and stabilize the distorted triptycene structure.

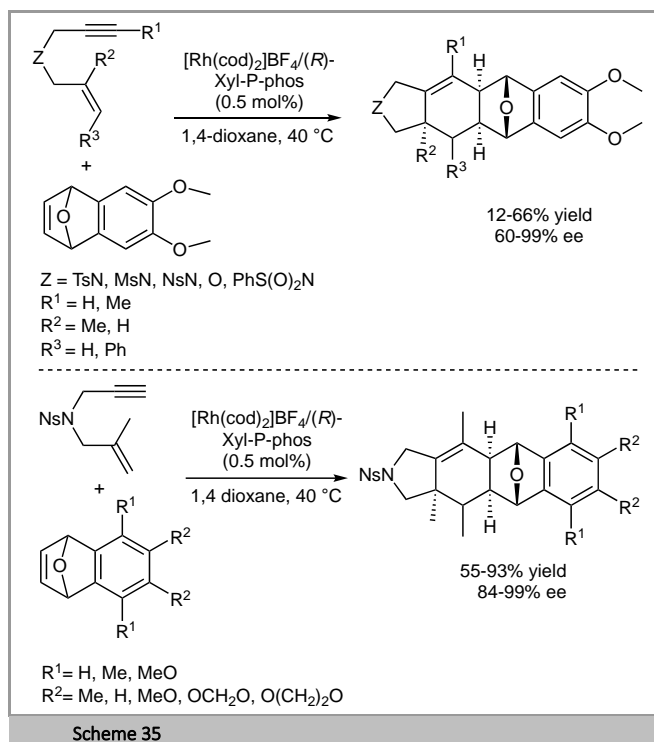


In 2018, Mata, Mischne and co-workers reported the [2+2+2] cycloaddition reactions utilizing immobilized alkynes with soluble 1,6-diyne-esters to access the simultaneous preparation of soluble and solid-supported phthalides (Scheme 34).⁹⁵ The reactions were performed with 5 mol% of RhCl(PPh₃)₃ in toluene at reflux for 2 h. This approach was applied to generate soluble and immobilized substituted phthalides by means of a process integrating solution and solid-phase synthesis. To face limitations of the formation of

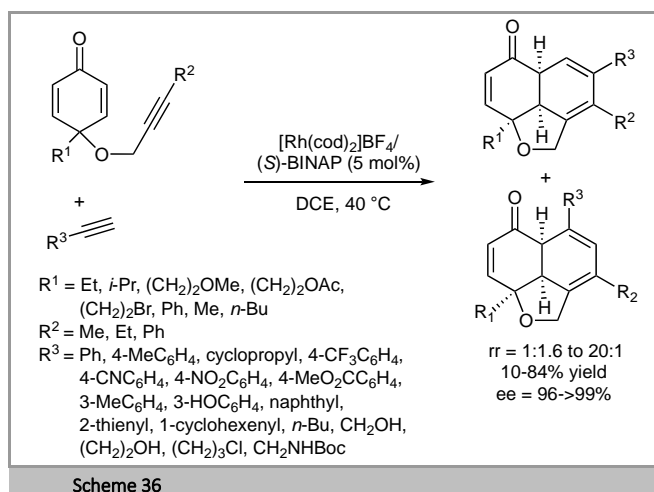
homodimers, the authors immobilized the monoalkynes to a solid support, prepared from Merrifield resin, to form homodimers in solution-phase which can be easily separated by simple filtration. Resin-bound cross-cycloadducts can be cleaved from the solid support by an appropriate reagent. Side by side solid and solution-phase synthesis of phthalides via [2+2+2]-cycloadditions were performed with moderate regioselectivities comparable to those obtained in homogeneous media but with a better separation of the cycloadducts. Released products cleaved from immobilized phthalides were prepared in 40-70% overall yield. Better regioselectivities were reached by using 20 mol% of Cp*RuCl(cod) at 128 °C for 4 h with regioselectivities up to 14:1 for resin-bound products vs up to 13:1 for solution-based products.



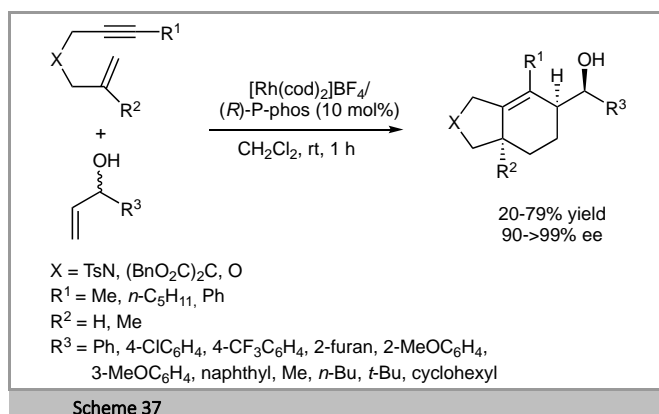
In 2019, Fan, Zhou and co-workers established the Rh-catalyzed asymmetric [2+2+2] cycloaddition of 1,6-enynes and oxabenzonorbornadienes to access polycyclic compounds in 12-66% yield and 60-99% ee (Scheme 35).⁹⁶ The reaction was carried out in the presence of [Rh(cod)₂]BF₄ (0.5 mol%) as the rhodium precursor and (*R*)-Xyl-P-Phos as a ligand in 1,4-dioxane at 40 °C, and delivered a range of polycyclic cycloadducts bearing quaternary stereocenters. 1,6-Enynes having a nitrogen- or oxygen-tether were well tolerated whereas carbon-linked 1,6-enyne or 1,7-enyne failed to afford the expected cycloadducts, and the use of internal alkynes and alkenes led to lower yields. A range of oxabenzonorbornadienes with electron-donating or withdrawing groups in various positions of the aryl ring could be used in the reaction, affording enantioselectivities of 84-99%.



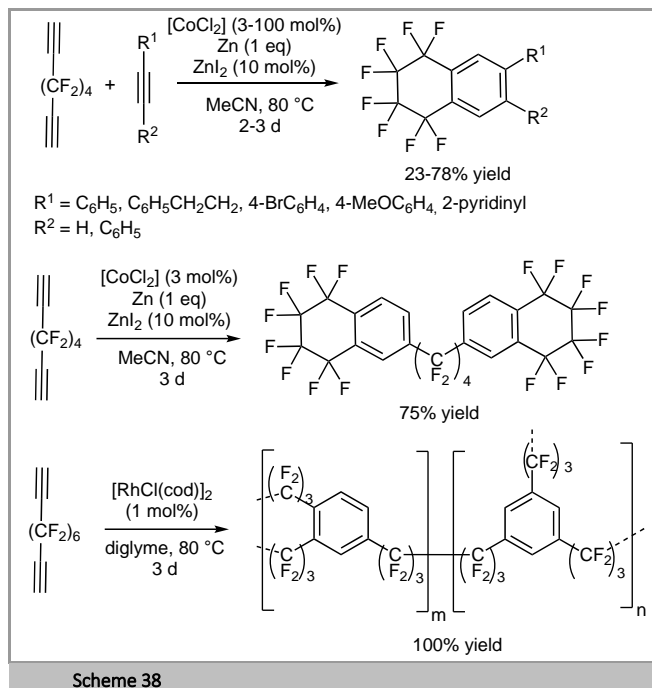
In 2020, Xu and co-workers developed an enantioselective Rh(I)-catalyzed [2+2+2] cycloaddition of cyclic 1,6 enynes with terminal alkynes to provide fused tricyclic hydronaphthofuran scaffolds having three contiguous stereocenters (Scheme 36).⁹⁷ The reaction was best performed with [Rh(cod)₂]BF₄/(*S*)-BINAP (5 mol%) as a catalyst at 40 °C in DCE for a range of terminal alkynes and enynes having aliphatic or phenyl groups on the quaternary carbon center to afford the desired hydronaphthofuran derivatives in 10-84% yield and enantiomeric excess values ranging from 96% to >99%. This desymmetric [2+2+2] cycloaddition was sensitive to steric hindrance that governed both the regioselectivity and the reactivity, with the formation of the other regioisomer observed when replacing the methyl group on the quaternary carbon center of the enyne with an ethyl substituent, whereas a lower yield of 10% was obtained when a phenyl-substituted enyne was used. Nitrogen-tethered enynes were also efficient for this reaction (not shown).



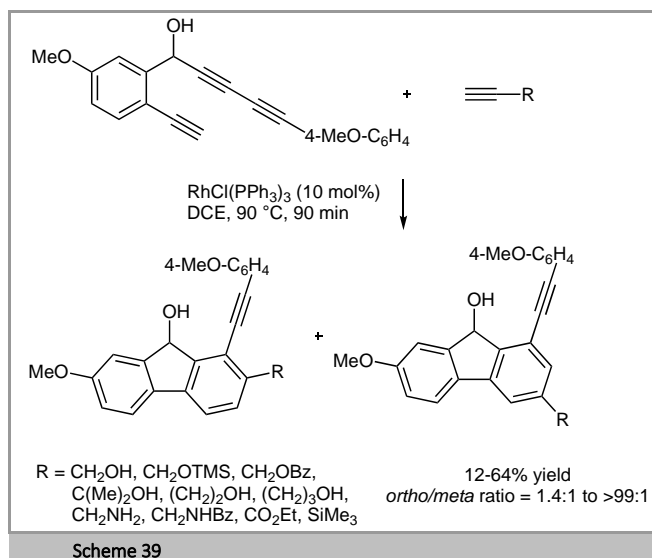
In 2020, Tanaka and co-workers described the rhodium-catalyzed asymmetric [2+2+2] cycloaddition of 1,6-enynes with racemic secondary allylic alcohols. The reaction of various enynes with 5 equiv of a racemic secondary allylic alcohol proceeded at room temperature in the presence of $[\text{Rh}(\text{cod})_2]\text{BF}_4$ as the rhodium source and (*R*)-P-phos as a ligand to afford, through a kinetic resolution of the alcohol, the corresponding bicyclic cyclohexenes bearing three stereocenters, as single diastereomers in 20–79% yield and 90–>99% ee (Scheme 37).⁹⁸ Various alkyl or aryl substituents were tolerated on the enyne partner whereas for the allylic alcohol, 1-phenyl-prop-2-en-1-ol derivatives having electronically and sterically diverse substituents on the benzene ring were suitable.



In 2020, Agou, Fukumoto, Kubota and co-workers reported the preparation of α,ω -diynes bearing a perfluoroalkylene linker and their use in Co- or Rh-catalyzed [2+2+2] cycloaddition reactions. The $-(\text{CF}_2)_4-$ tethered α,ω -diyne reacted with diversely substituted alkynes in the presence of $[\text{CoCl}_2]$ (3–100 mol%), Zn (1 equiv) and ZnI_2 (10 mol%) at 80 °C to provide benzene derivatives fused with an octafluorocyclohexene moiety in 23–78% yield (Scheme 38).⁹⁹ Trimerization of this α,ω -diyne could also be performed in 75% yield with 3 mol% of the catalyst. On the other hand, the $-(\text{CF}_2)_6-$ tethered α,ω -diyne was polymerized in the presence of $[\text{RhCl}(\text{cod})]_2$.



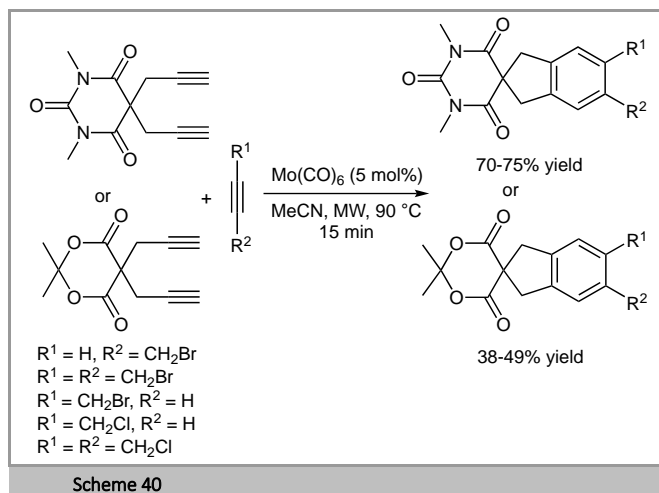
In 2021, Kotora and co-workers described an efficient route to access the selaginpulvilins scaffold through a [2+2+2] cyclotrimerization reaction. The reaction was performed with a triyne in the presence of 10 mol % of $\text{RhCl}(\text{PPh}_3)_3$ in DCE at 90 °C in 12–64% yield (Scheme 39). The scope of the cycloaddition of triynes with diversely functionalized internal alkynes was examined. The cycloaddition proceeded with a high *ortho* regioselectivity up to 13.1:1 in reasonable yields. Internal alkynes such as 3-hexyne, diphenylethyne, but-2-yn-1-ol and but-2-yne did not react. This strategy allowed to access the key intermediates having the 1-alkynylfluorenone scaffold of selaginpulvilins. A mechanistic rationale was proposed to explain the regioselectivity.¹⁰⁰



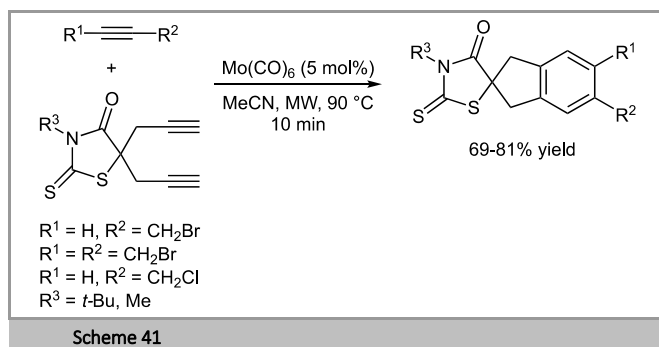
2.2.2. Molybdenum-Catalyzed [2+2+2] Cycloaddition

In 2018, Kotha and co-worker described the Mo-catalyzed [2+2+2] cycloaddition of propargyl halides with 1,6-diyne to

prepare benzyl halide derivatives of barbituric acid and Meldrum's acid derivatives containing a spiro linkage (Scheme 40).¹⁰¹ The authors used $\text{Mo}(\text{CO})_6$ (5 mol%) as a catalyst under microwave irradiation in acetonitrile at 90 °C to access the desired halomethyl benzene derivatives in 70-75% yield. On the other hand, Meldrum's acid derived cycloadducts were formed in 38-49% yield along with the self-dimerized product (12-15% yield).

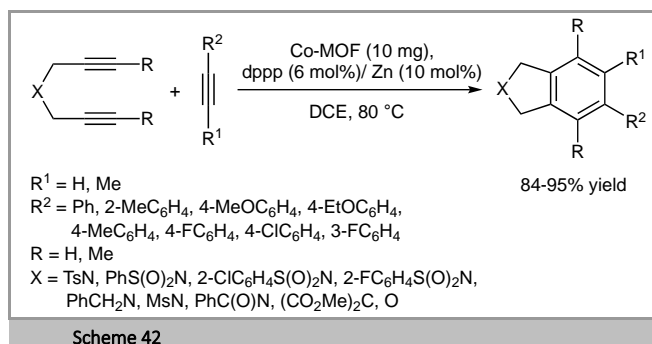


The same authors extended this Mo-catalyzed [2+2+2] cyclotrimerization to the synthesis of spirorhodanines by using dipropargyl derivatives with propargyl halides as partners under microwave irradiation. The corresponding spirocyclic compounds were obtained in 69-81% yield (Scheme 41).¹⁰²

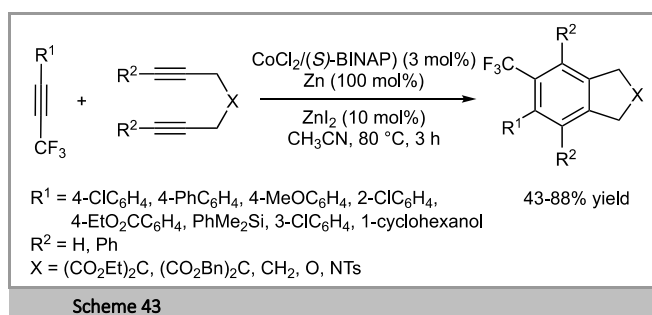


2.2.3. Cobalt-Catalyzed [2+2+2] Cycloaddition

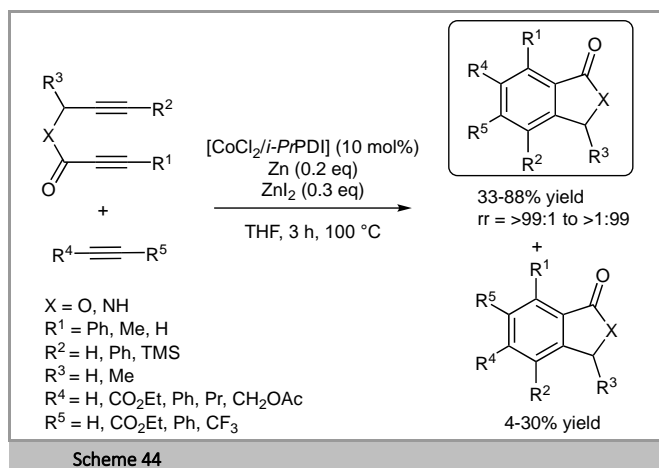
In 2018, Du, Liu and co-workers developed a cobalt-based metal-organic framework (MOF) catalyst for the [2+2+2] cycloaddition of diynes and alkynes to access highly substituted benzenes (Scheme 42).¹⁰³ The reaction proceeded in the presence of the Co-MOF catalyst (10 mg), dppp (6 mol%) and Zn powder (10 mol%) in DCE at 80 °C for a range of phenyl acetylenes bearing electron-donating or -withdrawing groups, and nitrogen-, carbon- or oxygen-tethered diynes to give the substituted benzene derivatives in 84-95% yield. The Co-MOF heterogeneous catalyst could be recycled five times without loss of activity.



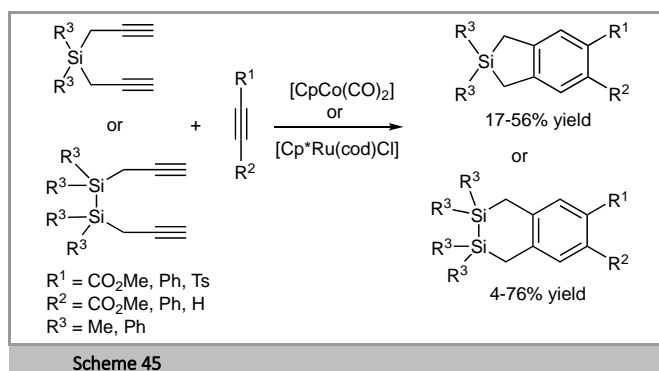
In 2018, Konno and co-workers described a cobalt-catalyzed [2+2+2] cycloaddition of fluorinated internal alkynes with 1,6 diynes to access variously substituted fluoroalkylated benzene derivatives (Scheme 43).¹⁰⁴ The reaction was best carried out in the presence of $\text{CoCl}_2/(S)\text{-BINAP}$ (3 mol%), Zn (100 mol%), ZnI_2 (10 mol%) at 80 °C in acetonitrile to provide the desired bicyclic aromatic compounds in 43-88% yield.



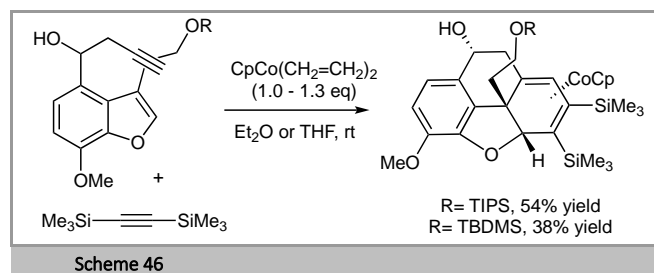
In 2020, Savela and co-workers reported the preparation of isobenzofuranones and isoindolinones through cobalt-catalyzed [2+2+2] cycloaddition of diynes with alkynes (Scheme 44).¹⁰⁵ The reaction used $[\text{CoCl}_2]$ (10 mol%) and a sterically hindered tridentate pyridine-2,6-diimine, *i*PrPDI, as a ligand, in the presence of Zn (0.2 equiv), ZnI_2 (0.3 equiv) at 100 °C in THF. Ester, methyl, phenyl and alkyl substituents on the alkynes were well tolerated for this cobalt-catalyzed [2+2+2] cycloaddition of ester or amide tethered 1,6-diynes, delivering the corresponding isobenzofuranones and isoindolinones in 4-88% yield and regioselectivities varying from >99:1 to >1:99. The regioselectivities observed for the formation of isoindolinones were higher with an amide link as compared to an ester tether, and the preferred regioisomers were mainly the ones having the bulky substituent in *ortho* position to the most electron-withdrawing group.



In 2020, Kabe and co-workers described the $[\text{CpCo}(\text{CO})_2]$ and $[\text{Cp}^*\text{Ru}(\text{cod})\text{Cl}]$ -catalyzed $[2+2+2]$ cycloaddition of bispropargyl silanes and disilanes with alkynes to form benzo-2-silaindanes and benzo-2,3-disilatetralines, respectively (Scheme 45).¹⁰⁶ The low reactivity of these diynes led to poor yields and competitive dimerization and trimerization of the alkynes were mainly observed. The use of $[\text{CpCo}(\text{CO})_2]$ led to low yields for both electron-rich and electron-deficient alkynes whereas $[\text{Cp}^*\text{Ru}(\text{cod})\text{Cl}]$ gave moderate yields for electron-deficient partners and no reaction or low yields for electron-rich alkynes. Based on these results, the authors suggested different mechanistic pathways were involved for the $\text{CpCo}(\text{I})$ - and $\text{Cp}^*\text{Ru}(\text{II})\text{Cl}$ -catalyzed cycloadditions of siladiynes with alkynes: $[\text{CpCo}(\text{CO})_2]$ proceeded via a heterolytic coupling pathway to form cobaltacyclopentadiene and $[\text{Cp}^*\text{Ru}(\text{cod})\text{Cl}]$ proceeded via a homolytic coupling pathway to give ruthenacyclopentatriene.

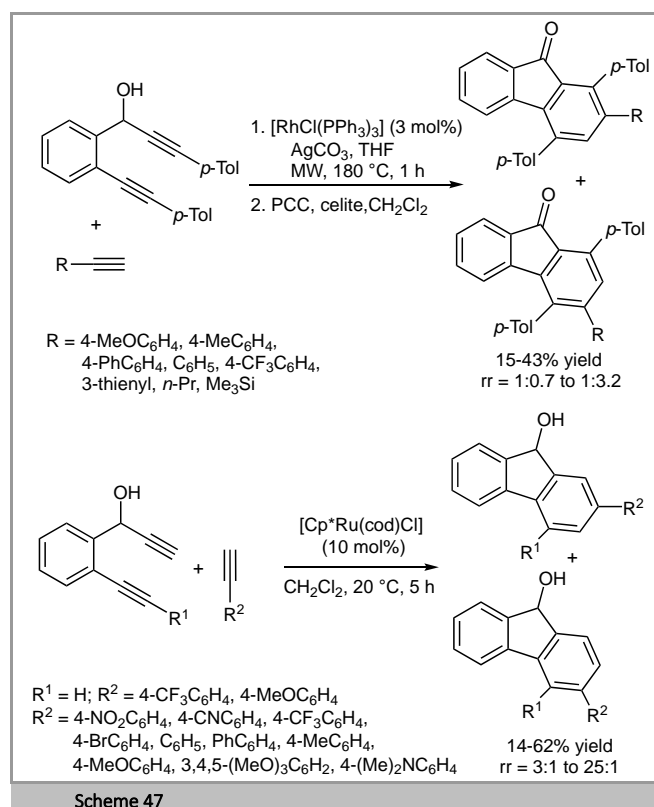


Vollhardt and co-workers studied the CpCo -mediated $[2+2+2]$ cycloaddition of alkynes to the 2,3-double bond of benzo[*b*]furans to prepare Co -complexed tetrahydrophenanthro[4,5-*bcd*]furans as a potential route toward morphinan substructures (Scheme 46).¹⁰⁷ The reaction proceeded with high levels of diastereoselectivity but lacked regioselectivity when unsymmetrical alkynes were used instead of bis(trimethylsilyl)acetylene. The authors also showed that the $[2+2+2]$ cycloaddition of benzo[*b*]thiophenes with $\text{CpCo}(\text{CH}_2=\text{CH}_2)_2$ led to the corresponding Co -complexed tetrahydrophenanthro[4,5-*bcd*]thiophens in moderate yields.

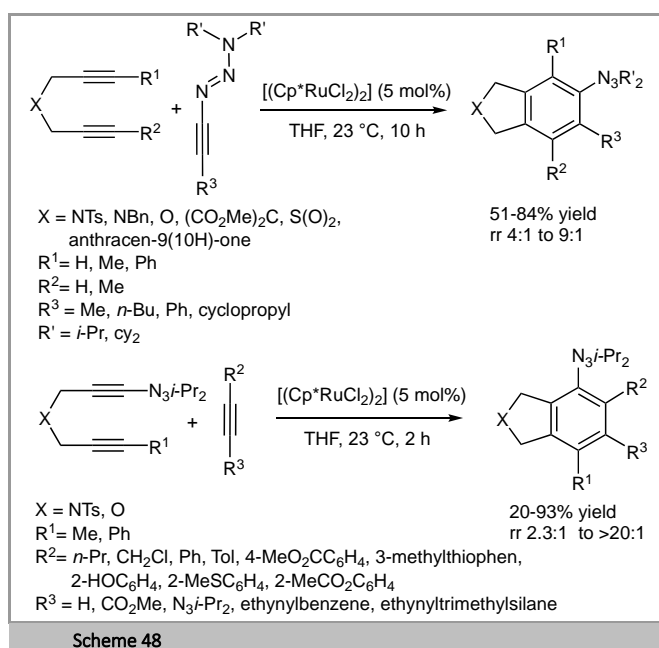


2.2.4. Ruthenium-Catalyzed $[2+2+2]$ Cycloaddition

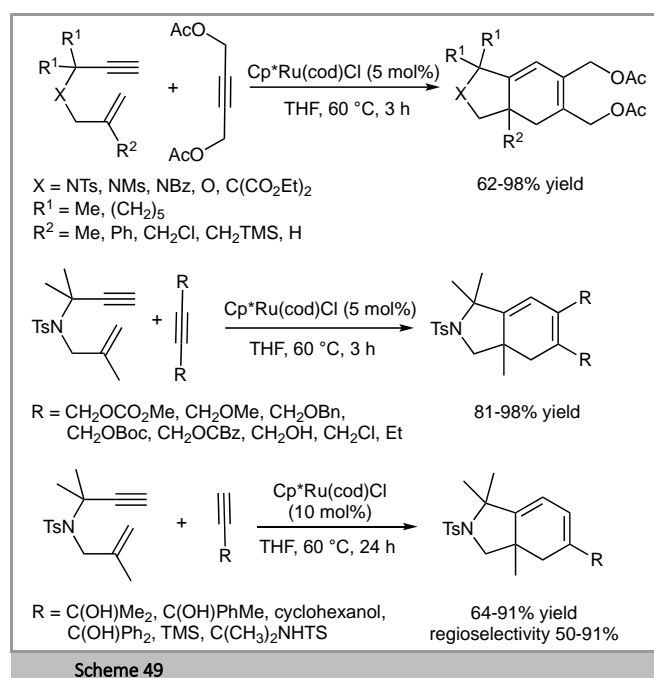
Kotora and co-workers reported the synthesis of tri- and disubstituted fluorenols through $[2+2+2]$ cyclotrimerization of mono- and disubstituted diynes with terminal alkynes. For the formation of disubstituted fluorenols, the authors showed that the 2,4-regioisomers were preferentially formed with $[\text{Cp}^*\text{Ru}(\text{cod})\text{Cl}]$ as a catalyst whereas Rh complexes led to the 3,4-regioisomers as the major products. The use of Wilkinson's catalyst $[\text{RhCl}(\text{PPh}_3)_3]$ in the presence of Ag_2CO_3 under microwave irradiation allowed, after oxidation of the crude fluorenols with PCC , the preparation of the corresponding fluorenones in 15-43% yield, with regioisomeric ratios (rr) of 1:0.7 to 1:3.2 (Scheme 47). On the other hand, a range of 2,4-disubstituted fluorenols were prepared through Ru -catalyzed $[2+2+2]$ cyclotrimerization under mild reaction conditions and high functional group tolerance by using $[\text{Cp}^*\text{Ru}(\text{cod})\text{Cl}]$ (10 mol%) as a catalyst in dichloromethane at 20 °C. The desired products were obtained in 14-62% yield with rr values varying from 3:1 to 25:1. These compounds were further converted in three steps into the corresponding spirobifluorenes (not shown).¹⁰⁸



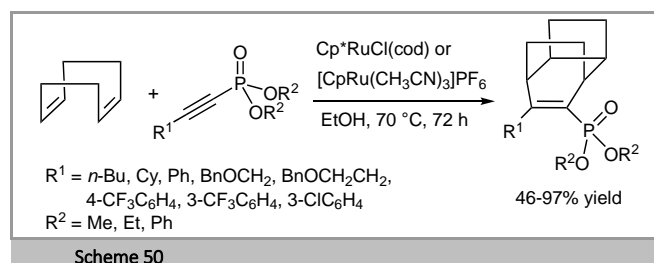
In 2019, Cramer, Severin and co-workers developed an efficient divergent synthesis of densely substituted aryl and pyridyl triazenes via Cp*Ru-catalyzed [2+2+2] cyclotrimerization reactions of both simple alkynyl triazenes and tethered 1-diyne triazenes (Scheme 48).¹⁰⁹ The triazene group induced a high regioselectivity and the [Cp*RuCl₂]₂-catalyzed reaction generally afforded the more sterically hindered product (up to >20:1 rr) in yields ranging from 20 to 93%. Interestingly, replacing an alkyne with a nitrile allowed formation of the pyridine derivatives (not shown). The substituted fused aromatic triazenes thus obtained could be readily functionalized through the versatile triazene group installed on the aryl or pyridyl ring whereas intramolecular reactions afforded a variety of valuable heterocycles.



Tenaglia and co-workers described the crossed intermolecular [Cp*Ru(cod)Cl]-catalyzed [2+2+2] carbocyclization reactions of 1,6-enynes with unactivated alkynes to prepare bicyclohexa-1,3-dienes containing a quaternary center at the ring junction (Scheme 49).¹¹⁰ Using 5-10 mol% of [Cp*Ru(cod)Cl], the reaction of 1,6-enynes with internal alkynes afforded the ring-fused cyclohexadienes in 62-98% yields and was tolerant to a wide range of functional groups. Terminal alkynes could be used in this transformation as well and the regioselectivity of the reaction was controlled by increasing the steric bulk at the propargyl carbon atom(s) of the reactants.



In 2019, Tam and co-workers reported the Ru-catalyzed [2+2+2] bis-homo-Diels-Alder cycloaddition of 1,5-cyclooctadiene with alkynyl phosphonates to access tricyclo[4.2.2.0]dec-7-ene tricyclic compounds (Scheme 50). In the presence of [Cp*Ru(cod)Cl] or [CpRu(CH₃CN)₃]PF₆, the reaction afforded the desired cycloadducts in 46-97% yield and was tolerant to steric bulk on both the phosphonate and the alkynyl moieties.¹¹¹

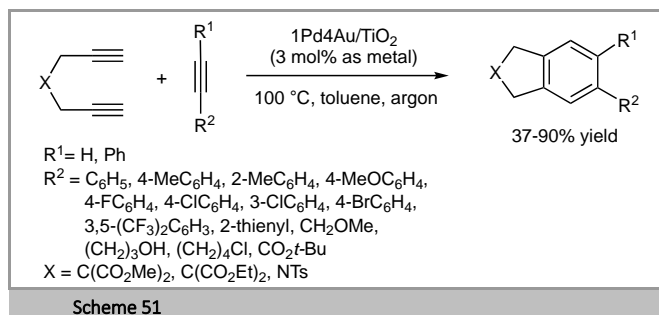


Tomás-Gamasa, Mascareñas and co-workers reported in 2020 the intracellular ruthenium-catalyzed (2+2+2) intramolecular and intermolecular cycloadditions of diynes with alkynes.¹¹² The authors showed for the first time the feasibility of multicomponent alkyne cycloaromatizations inside live mammalian cells with Ru-catalysts and were able to synthesize biorelevant polycyclic compounds such as anthraquinone skeletons from simple precursors inside cells.

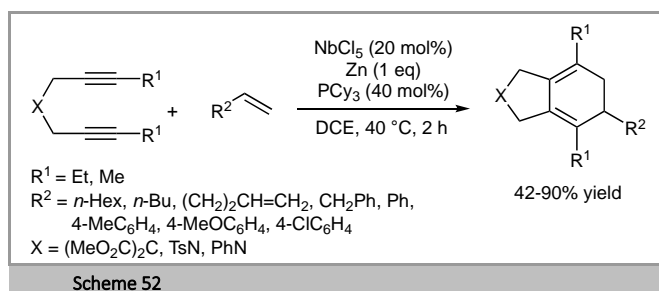
2.2.5. Other Metal-Catalyzed [2+2+2] Cycloaddition

In 2018, Shishido, Miura and co-workers reported the [2+2+2] cycloaddition reaction of substituted alkynes over supported Pd-Au alloy catalysts prepared through a sol-immobilization method (Scheme 51).¹¹³ The authors showed that the Pd/Au ratio was a crucial factor for the catalytic activity and the compatibility of this catalyst with open-air conditions. Notably, the 1Pd4Au/TiO₂ catalyst was highly air-tolerant and allowed the [2+2+2] cross-cycloaddition of 1,6-diyne with alkynes on a wide substrate scope with yields ranging from 59%

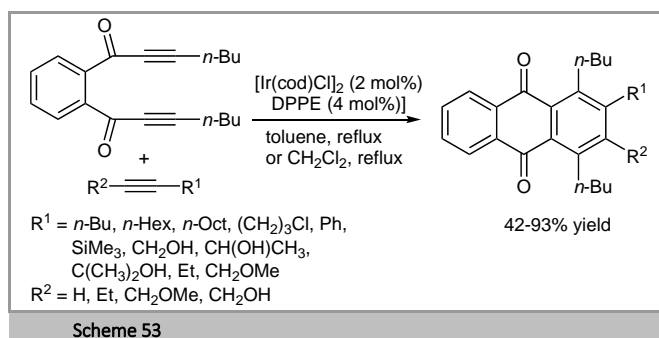
to 90%. Intramolecular cycloaddition of triynes was also performed using 1Pd3Au/TiO₂ catalyst. High reusability was observed for the supported Pd-Au alloy catalyst which could be reused in four consecutive catalytic tests without significant decreases in yields.



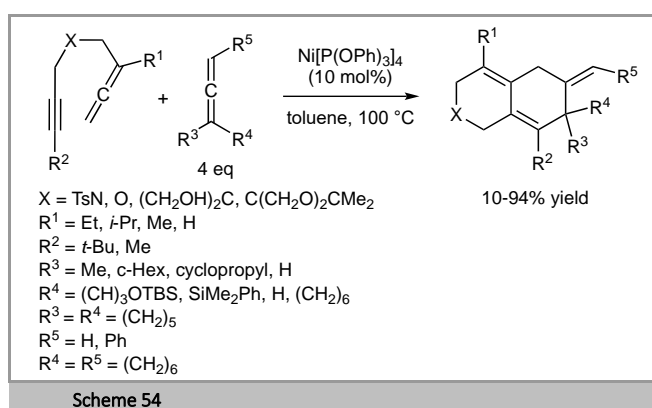
Obora and co-workers developed a NbCl₅, Zn, and PCy₃ catalytic system for the [2+2+2] cycloadditions of diyynes and simple alkynes to form bicyclic cyclohexadienes without C=C bond migration, in yields ranging from 42% to 90% (Scheme 52).¹¹⁴ The reaction was catalyzed by low-valent Nb species generated in situ and the authors showed that the presence of a phosphine ligand was critical for its stabilization. Various aliphatic and aromatic alkenes were tolerated but internal alkenes did not give the desired cycloadducts.



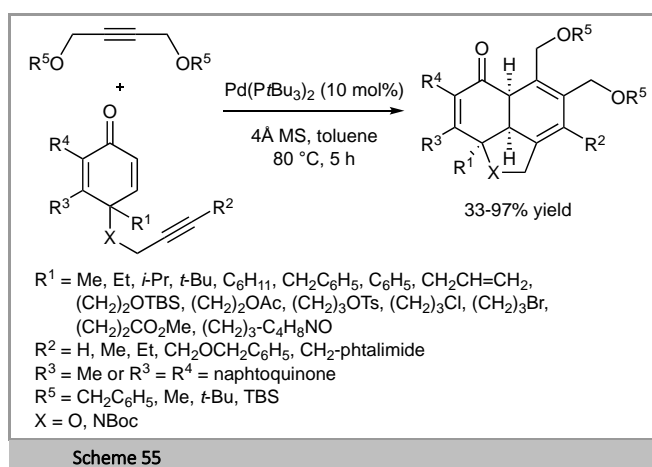
Takeuchi and co-workers described the iridium-catalyzed [2+2+2] cycloaddition of a 1,2-bis(propioyl)benzene derivative with terminal and internal alkynes to form anthraquinones.¹¹⁵ The reaction was carried out in the presence of [Ir(cod)Cl]₂ (2 mol%) and DPPE (4 mol%) in either refluxing toluene for terminal alkynes or refluxing dichloromethane for internal alkynes, to afford the desired cycloadducts in yields ranging from 42% to 93% (Scheme 53). The authors also prepared a fluorenone in 94% yield by iridium-catalyzed [2+2+2] cycloaddition using [Ir(cod)Cl]₂/F-DPPE as a catalytic system.



In 2019, Arai and co-workers developed a highly site-, regio- and stereoselective Ni-catalyzed [2+2+2] cycloaddition reaction between allene-ynes and various mono-, di- and tri-substituted allenes to give highly functionalized carbocycles (Scheme 54).¹¹⁶ The reaction was performed in the presence of Ni[P(OPh)₃]₄ (10 mol%) in toluene at 100 °C and delivered regioselectively the bicyclic structures in yields varying from 10% to 94% for oxygen-, nitrogen- and carbon-tethered allene-ynes. The reaction with a cyclic allene allowed the construction of a tricyclic system. The authors investigated the reaction mechanism by DFT calculations that revealed the selectivity-determining step was strongly affected by all of the substituents on π-components.

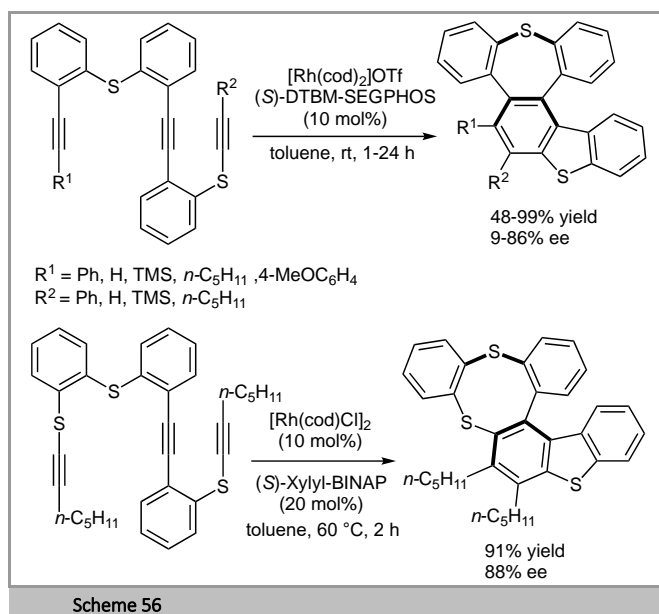


In 2021, Feng, Tian, He and co-workers reported the synthesis of tricyclic hydronaphthofuran and hydroxynaphthopyrrole derivatives through a palladium-catalyzed [2+2+2] cycloaddition. Internal alkynes and alkyne-tethered cyclohexadienones provided tricyclic compounds in the presence of 10 mol % Pd(*Pt*-Bu₃)₂ and 4Å molecular sieves at 80 °C in toluene (Scheme 55). The cycloadducts were obtained as single diastereomers in 33-97% yield. As alkyl-substituted alkynes were inefficient in this reaction, the authors suggested that the presence of the oxygen atom on the ether was mandatory for the transformation.¹¹⁷

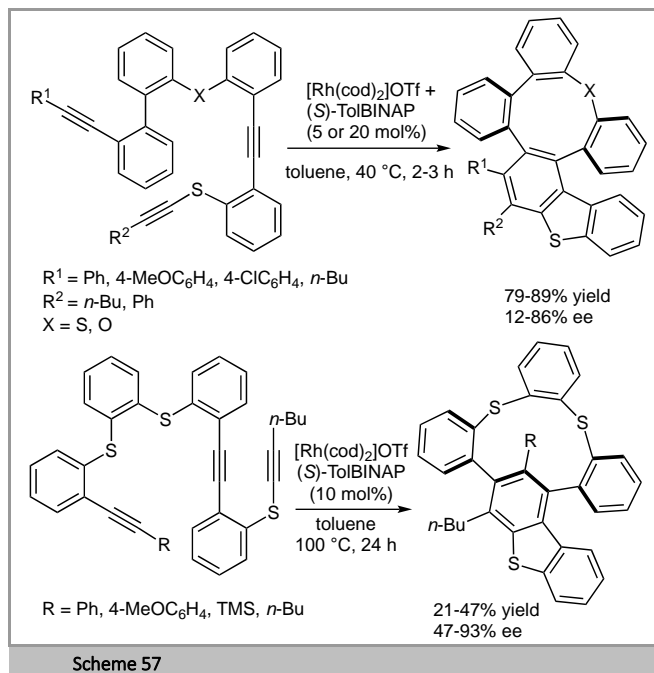


2.3. Totally Intramolecular [2+2+2] Cycloaddition Reactions

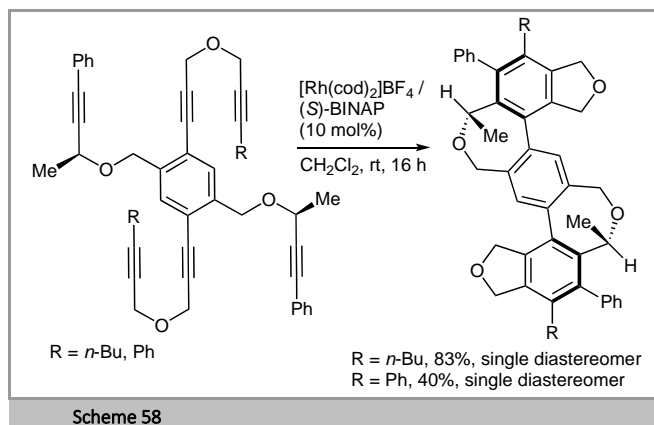
Shibata and co-workers described the rhodium-catalyzed enantioselective synthesis of sulfur-containing medium-ring heterocycles fused with an axially chiral biaryl moiety, through intramolecular [2+2+2] cycloaddition of triynes connected by sulfur-containing tethers (Scheme 56). Chiral tribenzothiepins and a tribenzodithiocin fused with benzothiophene were prepared in yields ranging from 48% to 99% and with enantioselectivities up to 88%, by using $[\text{Rh}(\text{cod})_2]\text{OTf}/(S)\text{-DTBM-SEGPHOS}$ and $[\text{Rh}(\text{cod})\text{Cl}]_2/(S)\text{-Xylyl-BINAP}$, respectively.¹¹⁸



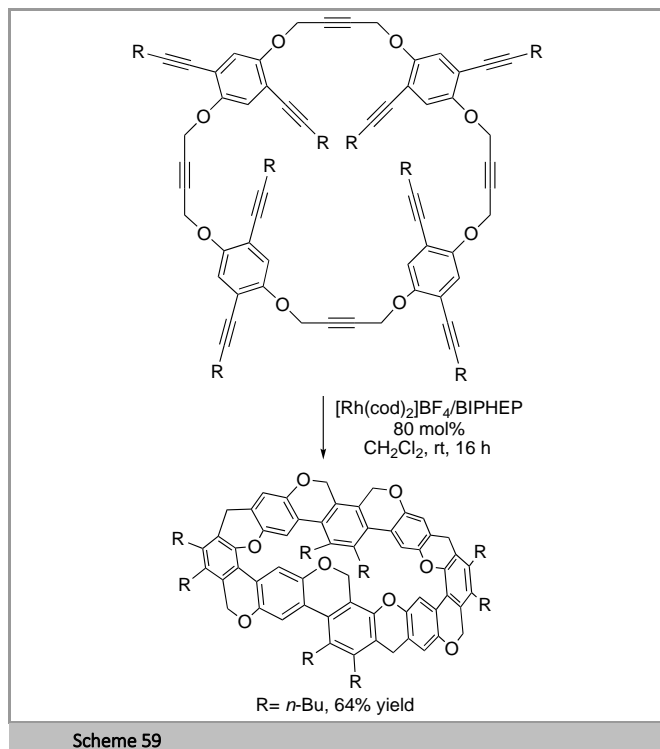
The same group extended this strategy to the synthesis of nine- to eleven membered cyclic polyphenylenes (Scheme 57).¹¹⁹ The enantioselective synthesis of tetrabenzothionines and a tetrabenzoxonine was achieved through Rh-catalyzed intramolecular [2+2+2] cycloaddition of triynes consisting of sulfur-tethered 1,6-diyne and S- or O-tethered 1,10-diyne moieties, respectively, in 21-89% yield and 12-93% ee. Interestingly, whereas the reaction of triynes consisting of 1,6-diyne and 1,11-diyne moieties having a sulfur tether led to eleven-membered metacyclophanes, the O- and S-tethered substrate afforded a tetrabenzo-1,4-oxathiecin with a ten-membered ring system.



In 2018, Tanaka and co-workers reported the rhodium-catalyzed diastereoselective intramolecular double [2+2+2] cycloaddition of chiral propargylic alcohol-derived hexaynes to access configurationally stable oxygen-linked Geländer-type *p*-terphenyls. The latter were obtained as single stereoisomers, the axial chirality being induced by the centrochirality of the chiral hexaynes (Scheme 58). The di-*n*-butyl- and diphenyl-substituted compounds showed efficient ultraviolet fluorescence and a relatively large absorption dissymmetry ratio.¹²⁰

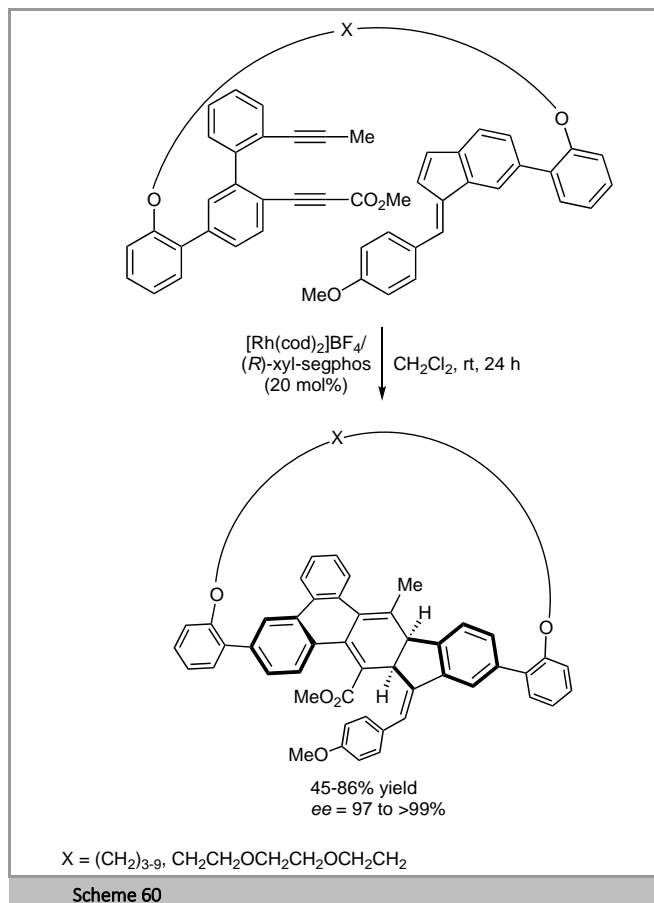


In 2019, the same group achieved the synthesis of a belt-shaped [8]cycloparaphenylene (CPP) and an enantioenriched Möbius-shaped [10]CPP by Rh-catalyzed intramolecular cyclotrimerizations of a cyclic dodecayne and a pentadecayne respectively. The use of the cationic complex $[\text{Rh}(\text{cod})_2]\text{BF}_4$ in combination with BIPHEP as a ligand allowed the highly effective intramolecular four sequential cyclotrimerizations of the cyclic dodecayne in 64% yield (Scheme 59) whereas the use of $(S)\text{-BINAP}$ as a ligand for the pentadecayne substrate afforded the Möbius-shaped [10]CPP compound in 95% ee after five sequential cyclotrimerizations.¹²¹



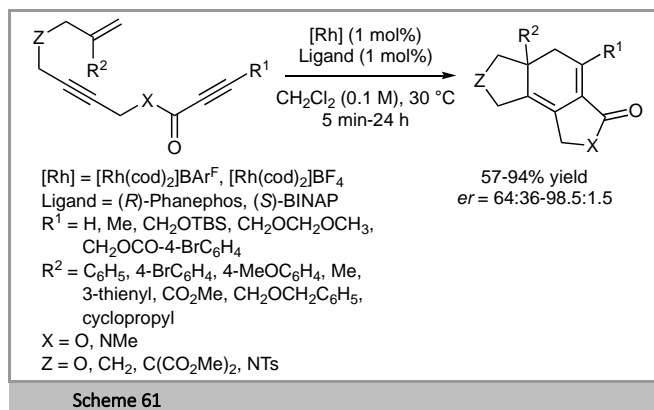
Scheme 59

In 2020, Tanaka and co-workers achieved the enantioselective synthesis of polycyclic aromatic hydrocarbon (PAH)-based planar chiral cyclophanes. The synthesis involved a cycloaddition of tethered diene-benzofulvenes and was performed in the presence of 20 mol % of $[\text{Rh}(\text{cod})_2]\text{BF}_4$ and (*R*)-xyl-segphos as a ligand at room temperature in CH_2Cl_2 . High selectivity was observed since the cycloadducts were obtained as single regioisomers in 45-86% yield. Yields ranging from 78% to 86% were obtained with moderate aliphatic chain-length (5 to 6 carbons) or when replacing alkyl chains by a PEG_3 moiety. Moreover, cyclic compounds were obtained with enantiomeric excesses of 97-99% ee. Interestingly, when (*S*)-xyl-segphos was used instead of (*R*)-xyl-segphos, the absolute configuration of the cycloadduct was reversed while an ee value of 98% was observed (Scheme 60).¹²²



Scheme 60

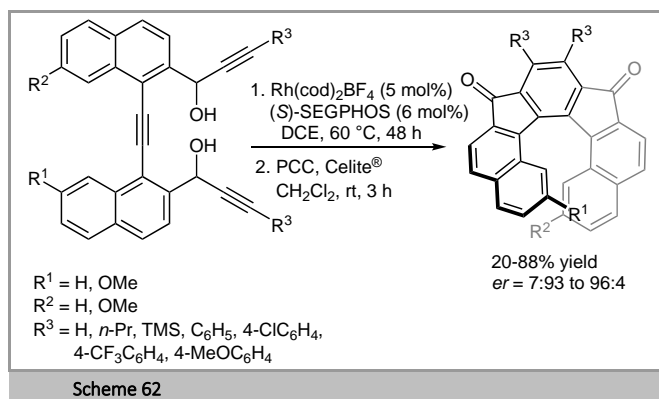
In 2021, Yasui, Yamamoto and co-workers developed an asymmetric Rh-catalyzed [2+2+2] cycloaddition of ene-yne-yne enediynes to produce chiral tricyclic cyclohexadienes. In the presence of 1 mol% of various rhodium catalysts and ligands in CH_2Cl_2 at 30 °C, tricyclic cycloadducts were formed in 57-94% yield with enantiomeric ratios up to 98.5:1.5 (Scheme 61). Interestingly, the authors showed that Rh-BINAP and Rh-Phanephos complexes did not follow the same mechanism: while Rh-BINAP complex can form a rhodacyclopentadiene intermediate as well as a rhodacyclopentene intermediate, Rh-Phanephos complex-catalyzed cycloaddition exclusively proceeded via a rhodacyclopentadiene intermediate. Consequently, Rh-Phanephos complex-catalyzed reactions did not allow substrates dimerizations.¹²³



Scheme 61

In 2021, Kotora and co-workers developed an enantioselective method for chiral [7]-helical dispirohydro[2,1-

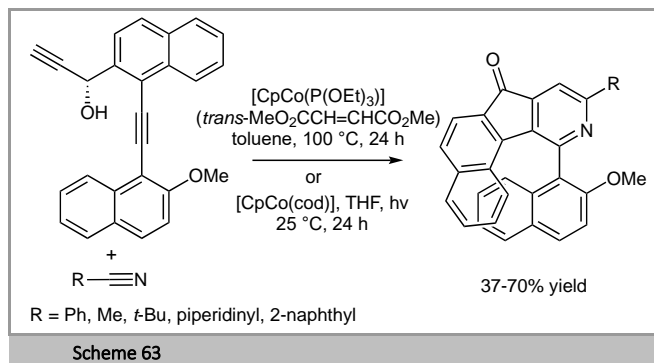
c]indeno[1,2-b]fluorene synthesis. The crucial step of this synthesis is an intramolecular enantioselective [2+2+2] cyclotrimerization of trienediols. In the presence of triynes, 5 mol% of $\text{Rh}(\text{cod})_2\text{BF}_4$ and 6 mol% of (*S*)-SEGPHOS in DCE at 60 °C for 48 h, helical diones were obtained in 20-88% yield and 7:93 to 96:4 enantiomeric ratios. Both (*S*)-SEGPHOS and (*R*)-SEGPHOS furnished the 4-methoxyphenyl helical dione in 70% and 53% yields with *er* values of 92:8 and 7:93, respectively. According to previous results of triynes cycloaddition giving helicenes, diynes with aromatic substituents furnished the corresponding cycloadducts in 53-88% yield and *er* values up to 96:4. In contrast, lower selectivities and yields were observed for alkyl and non-substituted triynes with 61:39 to 81:19 *er* values and 20-65% yield. Interestingly, when naphthyl groups supported one or two methoxy substituents, both yield and enantioselectivity decreased exhibiting 23-25% yield and 81:19 to 82:18 enantiomeric ratios (Scheme 62). These helical diones have been converted in 2 steps to [7]-helical dispirohydro[2,1-c]indeno[1,2-b]fluorenes which showed interesting photophysical properties including circularly polarized luminescence.¹²⁴



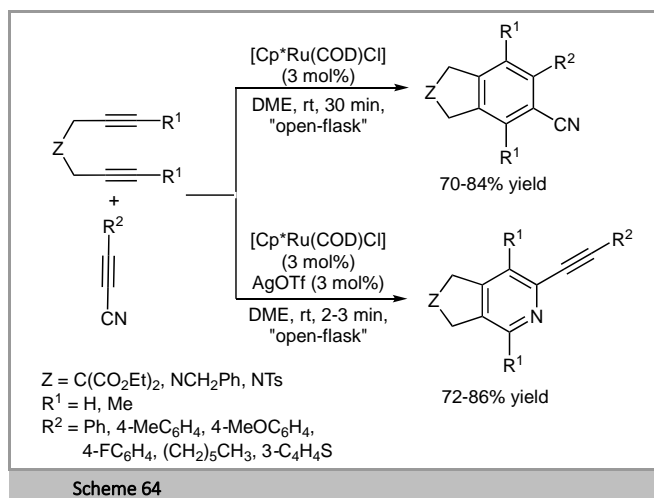
3. Formation of heterocycles

3.1. Cycloaddition of Alkynes with Nitriles

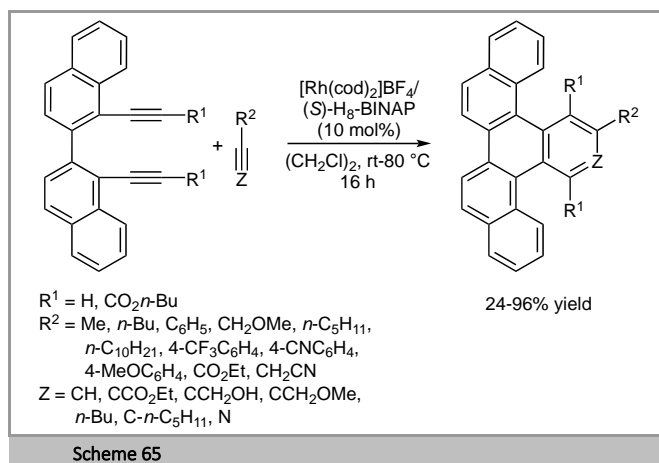
In 2018, Hapke and co-workers reported the synthesis of naphthylpyridines via cobalt-catalyzed [2+2+2] cyclotrimerization of a chiral diyne with nitriles. Either $[\text{CpCo}(\text{cod})]$ or $[\text{CpCo}\{\text{P}(\text{OEt})_3\}(\text{trans-MeO}_2\text{CCH}=\text{CHCO}_2\text{Me})]$ were used to prepare in 37-70% yield a series of racemic naphthylpyridines possessing configurationally stable biaryl axes, and resulting from the unexpected reoxidation of the chiral hydroxyl group to the ketone during the cyclization process (Scheme 63).¹²⁵



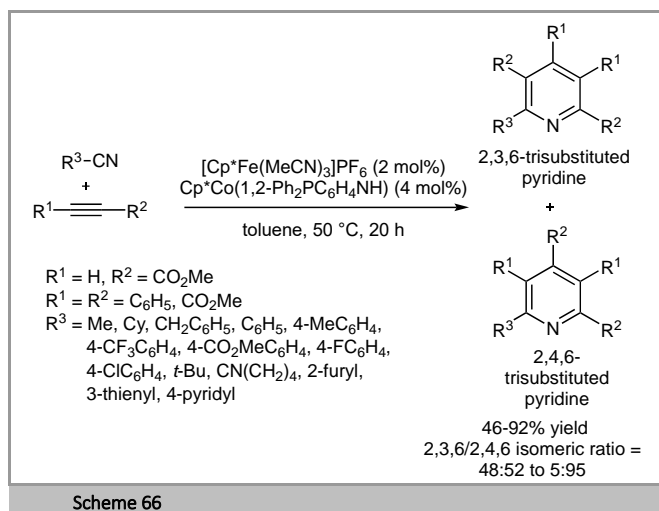
Goswami and co-workers described the chemoselective synthesis of fused cyanoarenes and 2-alkynylpyridines through ruthenium-catalyzed [2+2+2] cycloaddition of 1,6-diynes with alkynyl nitriles (Scheme 64).¹²⁶ The chemoselectivity of the reaction was shown to be additive-dependent; thus, by adding a catalytic amount of AgOTf to the $[\text{Cp}^*\text{Ru}(\text{cod})\text{Cl}]$ catalyst, the 2-alkynylpyridines were formed in 72-86% yield instead of the cyanoarenes that were obtained in the absence of the additive in 70-84% yield. The authors performed DFT calculations that indicated that a neutral ruthenium complex was involved in the formation of cyanoarenes, whereas the formation of 2-alkynylpyridines would rely on an *in situ* generated cationic Ru-complex.



Tanaka and co-workers described the synthesis of variously substituted benzopicenes and azabenzopicenes by rhodium-catalyzed [2+2+2] cycloadditions of binaphthyl-linked diynes with alkynes and nitriles. By using $[\text{Rh}(\text{cod})_2]\text{BF}_4/(\text{S})\text{-H}_8\text{-BINAP}$, the desired products were formed in 24-96% yield (Scheme 65) and the reaction could be applied to the synthesis of a benzopicene-based long ladder molecule as well as to the enantioselective synthesis of benzopicene-based helical molecules (not shown).¹²⁷ These compounds showed red shifts of absorption and emission maxima compared with the corresponding triphenylenes and azatriphenylenes.

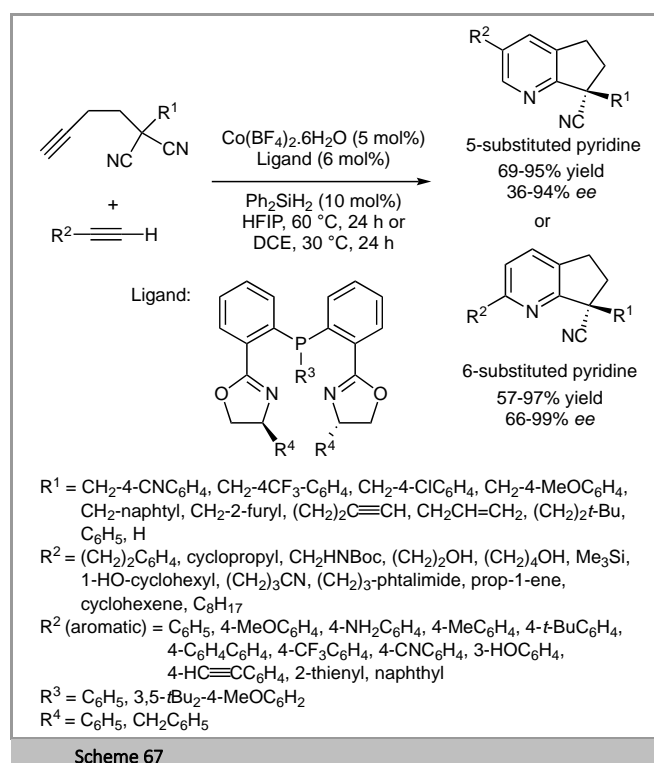


In 2020, Wang and co-workers succeeded in developing a heterocyclotrimerization of alkyne and nitriles supported by low cost transition metal co-catalysis. The reaction proceeded in the presence of 2 mol% of $[\text{Cp}^*\text{Fe}(\text{MeCN})_3]\text{PF}_6$ and 4 mol% of $\text{Cp}^*\text{Co}(1,2\text{-Ph}_2\text{PC}_6\text{H}_4\text{NH})$ in toluene at 50 °C. The cycloaddition reaction was significantly more efficient when electron-poor alkyne were considered. Nevertheless, other symmetrical alkyne gave the expected cycloadducts under the same conditions (Scheme 66). Unfortunately, the regioselectivity of the reaction was difficult to control when unsymmetrical alkyne were used, even for sterically hindered nitrile partners as the regioisomer ratio decreased down to 48:52. Reaction conditions were tolerant with different alkyls and aryl nitriles, delivering pyridine derivatives in 46-92% yield.¹²⁸

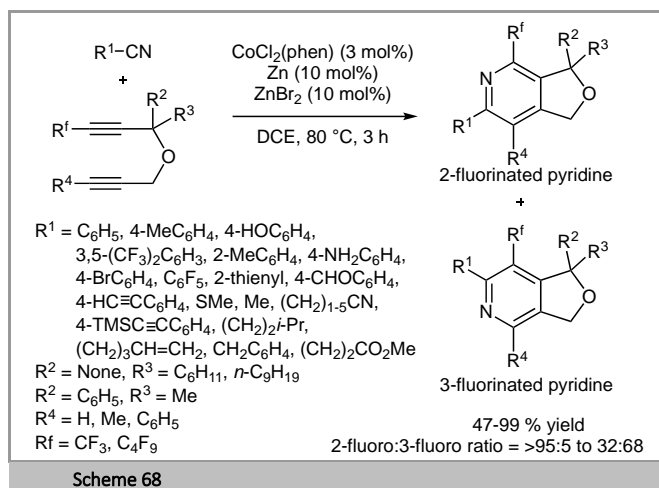


In 2021, Li and co-workers reported an efficient and enantioselective synthesis of pyridines with all-carbon quaternary centers. Alkyne and alkyne-tethered malononitriles gave the corresponding cycloadducts in the presence of 5 mol% of $\text{Co}(\text{BF}_4)_2 \cdot 6\text{H}_2\text{O}$, 6 mol% of ligand and 10 mol% of Ph_2SiH_2 for 24 h. When alkyl, alkenyl or silyl alkyne were engaged in the reaction at 60 °C in hexafluoroisopropanol, 5-substituted pyridines were produced in 36-95% yield and 86-94% ee. Interestingly, when the reaction was conducted in DCE at 30 °C with aryl alkyne, 6-substituted pyridines were obtained in 57-97% yield and 66-99% ee (Scheme 67). Although the reaction tolerated a broad substrate scope, the aryl substituent on the malononitrile gave significantly lower ee values of 36% and

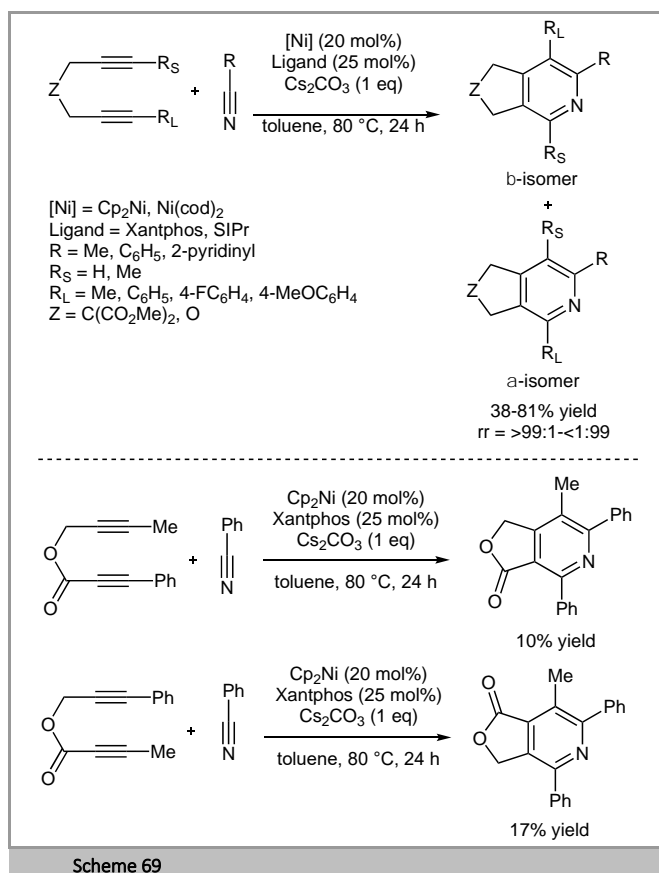
66% for 5-substituted and 6-substituted pyridines, respectively. Moreover, when the malononitrile supported a hydrogen as a substituent, the 6-substituted pyridine was obtained as a racemic mixture.¹²⁹



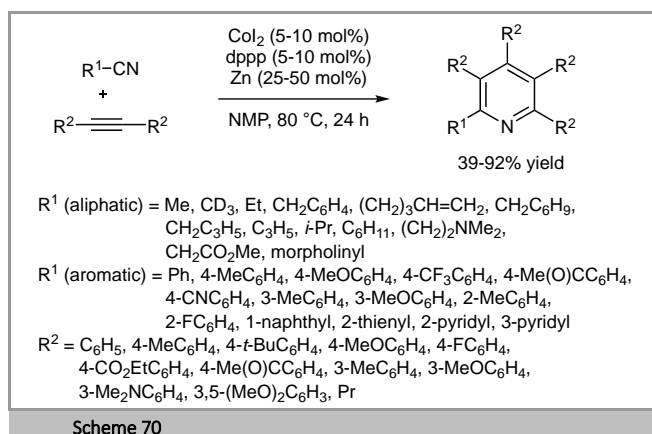
Considering the importance of trifluoromethyl-substituted heterocycles in pharmaceutical and agrochemical industries, Konno and co-workers reported in 2021 the preparation of fluorine-containing pyridines. The [2+2+2] cycloaddition reaction was performed using various alkyl/aryl nitriles and fluoro-substituted alkyne in DCE at 80 °C in the presence of 3 mol% of $\text{CoCl}_2(\text{phen})$, 10 mol% of zinc and 10 mol% of ZnBr_2 as catalysts. α -Fluoroalkylated pyridines were obtained in 47-99% yield (Scheme 68). A similar result was observed for the cyclization when a nonfluoroalkylated diyne was the partner instead of trifluoromethyl group. The authors also demonstrated that 2-fluoropyridines were exclusively obtained when using a terminal alkyne. However, 3-fluoropyridines could be obtained as major isomers when a bulkier group on the alkyne was considered.¹³⁰



In 2021, Seo, Hong and co-workers developed an efficient way to prepare functionalized pyridines through a [2+2+2] cycloaddition reaction between various symmetrical 1,6-diyne and nitriles. The reaction proceeded in toluene at 80 °C in the presence of cesium carbonate, using 25 mol% of a phosphine ligand and 20 mol% of an inexpensive nickel catalyst. The reaction could be run with no need of inert atmosphere. The same method has been applied to unsymmetrical 1,6-diyne to furnish pyridine derivatives in 38-81% yield (Scheme 69). As previously observed, the bulkier alkyne-substituent was found at the β -position with $\beta:\alpha$ ratio over 99:1. Dienes with aromatic substituents formed quasi-exclusively the α -isomer with a $\alpha:\beta$ ratios >99:1. When ester-linked diynes were used in this Ni-catalyzed cycloaddition, the aryl substituents were also found at the α -position with 10-17% yield.¹³¹

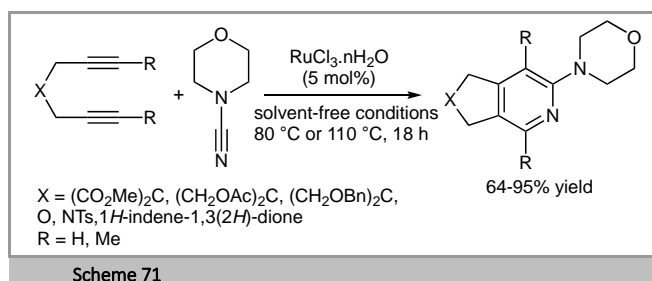


An efficient and versatile method to access penta-substituted pyridines was reported in 2021 by Wang, Yoshikai and co-workers. A fully intermolecular cycloaddition involving non-tethered alkynes and alkyl or aryl nitriles was achieved in the presence of 5-10 mol% of cobalt (II) iodide, 5-10 mol% of 1,3-bis-(diphenylphosphino)-propane and 25-50 mol% of zinc in NMP at 80 °C (Scheme 70). This inexpensive catalytic system has been employed leading to the corresponding polysubstituted pyridines in 39-92% yields. Moreover, the authors showed that the amount of catalyst could be decreased when alkyl nitriles instead of aryl nitriles were involved.¹³²



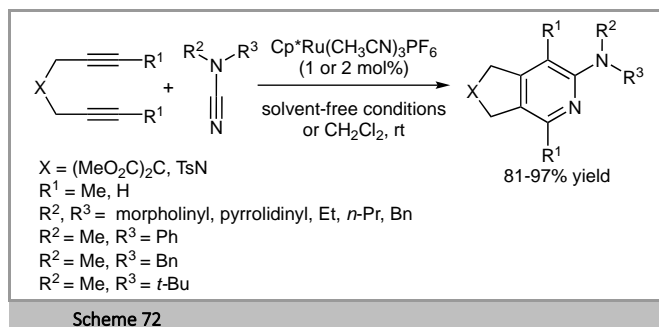
3.2. Cycloaddition of 1,6-Diyne with Cyanamides

In 2017, our group developed a straightforward environmentally sound approach to access functionalized 2-aminopyridines using a solventless Ru-catalyzed [2+2+2] cycloaddition of α,ω -diynes and cyanamides (Scheme 71). This green strategy involves [2+2+2] cycloaddition reaction at 80 °C or 110 °C in the presence of a stable, easy to handle and cost-effective RuCl₃·nH₂O complex (5 mol%) and provided the corresponding functionalized pyridine derivatives in yields up to 95%. This convenient atom-economical catalytic process carried out with non-toxic or volatile solvents tolerated a range of functionalities and offered significant advantage such as an operational simplicity allowing the construction of 2-aminopyridine scaffolds which are important building blocks for medicinal chemistry applications.¹³³

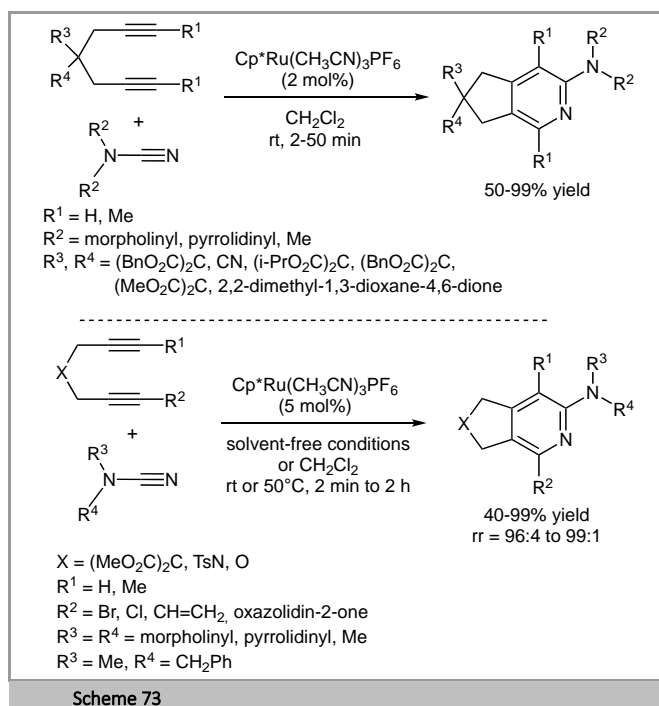


As far as 2-aminopyridine derivatives are concerned, only a few examples of [2+2+2] cycloaddition reactions of α,ω -diynes and cyanamides based on Ni, Co, Rh, Ir and Fe had been disclosed. In this context, we also described the same year, the novel Ru-catalyzed [2+2+2] cycloaddition reactions of α,ω -diynes and electron-rich nitriles under milder conditions, at

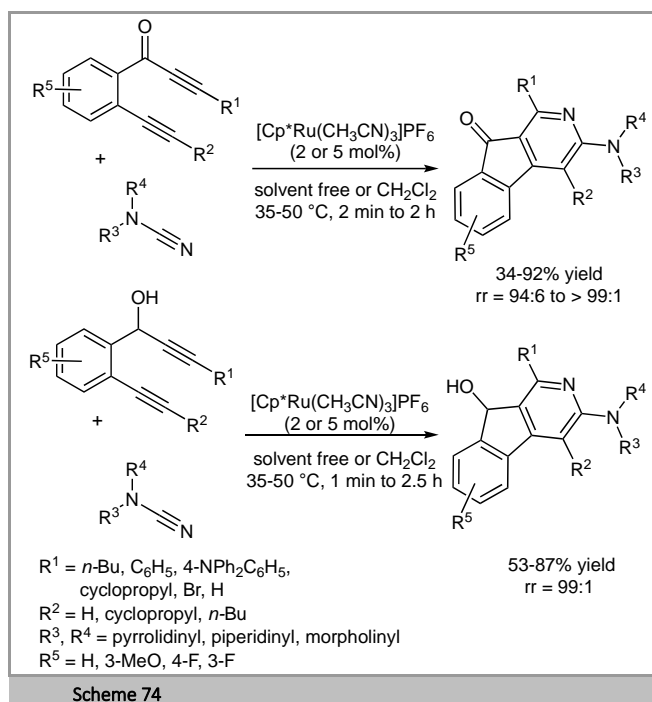
room temperature, using stable readily available $\text{Cp}^*\text{Ru}(\text{CH}_3\text{CN})_3\text{PF}_6$ complex at lower catalyst loading (1-5 mol%) with neither additional ligands nor additives, under solvent-free conditions or in dichloromethane (Scheme 72). This efficient mild transformation produced a wide range of annulated 2-aminopyridine cores of synthetic utility in yields up to 99% and excellent regioselectivities >99:1.¹³⁴



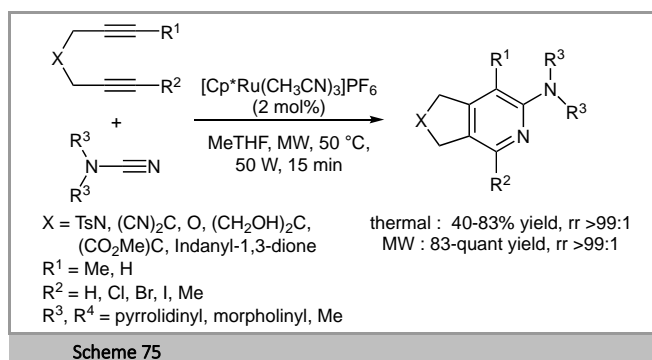
In a related study, this efficient process was extended in 2018 to a wide range of 1,6- and 1,7-diynes as well. In this survey, the catalytic performances of the commercially available $\text{Cp}^*\text{Ru}(\text{CH}_3\text{CN})_3\text{PF}_6$ were evaluated with neither additives nor ligands in a broad scope of novel substrates. The regioselective scalable atom-economical catalytic cycloadditions accommodated a range of symmetrical and unsymmetrical diynes which were reacted with cyanamides using 5 mol% of $\text{Cp}^*\text{Ru}(\text{CH}_3\text{CN})_3\text{PF}_6$ complex, under solvent-free conditions or in dichloromethane, at room temperature or 50 °C in yields up to 99% and up to 99:1 regioselectivities (Scheme 73). Application of the [2+2+2] cycloadditions to late-stage functionalizations of halo-containing adducts, using Pd- and Cu-catalyzed cross-coupling reactions, as well as cyanation and amination reactions, led to substituted 2-aminopyridines in 51-93% yield (not shown).¹³⁵



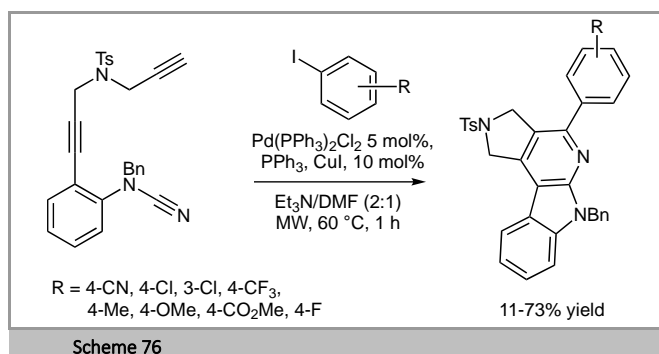
In 2018, our group reported an unexplored route to access fluorescent azafluorenone and azafluorenol derivatives (Scheme 74). The [2+2+2] cycloaddition of benzoyl-bridged 1,6-diynes with various cyanamides was performed using 2 or 5 mol% of $\text{Cp}^*\text{Ru}(\text{CH}_3\text{CN})_3\text{PF}_6$ at 35-50 °C in 34-94% yield and regioselectivities up to >99:1, mainly relied on the steric hindrance of the substituents on the terminus of the alkyne. Interestingly, photophysical properties of azafluorenones derivatives showed that these cycloadducts exhibited photoluminescence in the solid and liquid states with significant quantum yields.¹³⁶



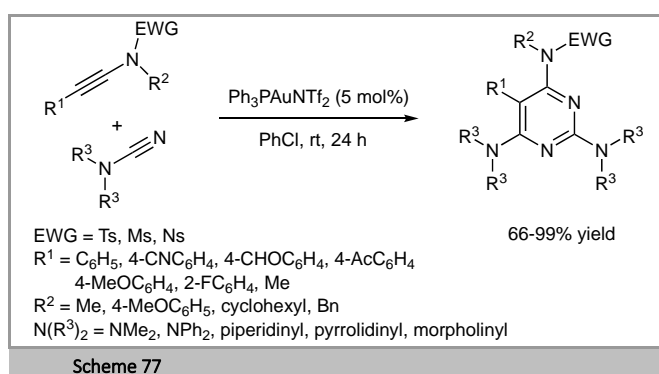
In 2019, we also demonstrated that the Ru-catalyzed cycloaddition reaction could efficiently occur under microwave irradiation (Scheme 75). This practical protocol led to diversely functionalized aminopyridines in up to quantitative yields and up to 99:1 regioselectivities. Higher yields were achieved in MeTHF at 50 °C under 50W in a shorter reaction time and with usually lower catalyst loading using $\text{Cp}^*\text{Ru}(\text{CH}_3\text{CN})_3\text{PF}_6$ catalyst (2 mol% vs 5 mol%) when comparing the microwave conditions to classical thermal conditions for the same [2+2+2] cycloaddition reactions. Furthermore, this sustainable method could be efficiently scaled-up demonstrating the usefulness of the protocol.¹³⁷



Mulcahy and co-workers developed the preparation of annulated 2-aryl- α -carboline heterocycles using transition metal catalysis through two approaches. A two-step synthesis relied on a sequential Sonogashira coupling/Rh-catalyzed [2+2+2] cyclotrimerization (not shown) whereas a second route involved a tandem Pd-catalyzed [2+2+2] cyclotrimerization to access the desired heterocycles in 11-73% yield (Scheme 76).¹³⁸ A comparison of the two approaches showed that the Pd-catalyzed one-pot procedure was less tolerant to functional groups and higher yields of 66-98% were obtained for the sequential route that used [Rh(cod)]₂BF₄/SEGPHOS for the cycloaddition step.



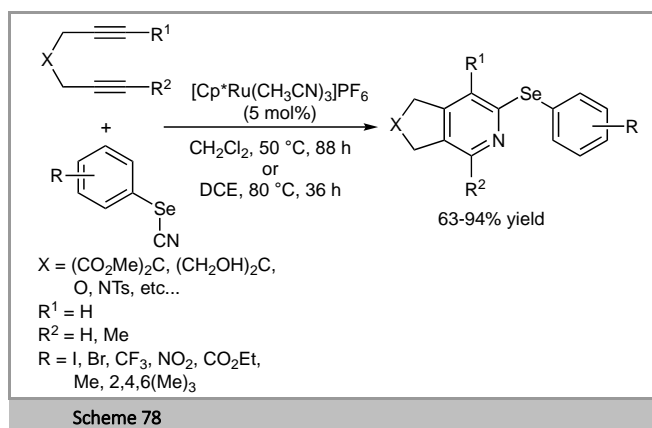
Kukushkin, Dubovtsev and co-workers reported the gold-catalyzed cycloaddition of cyanamides with ynamides to afford 2,4,6-triaminopyrimidines. Upon using Ph₃PAuNTf₂ (5 mol%) as a catalyst in chlorobenzene at room temperature, a range of diversely substituted 2,4,6-triaminopyrimidines were obtained from ynamides bearing various electron-withdrawing *N*-sulfonyl substituents, with alkyl or aryl groups as R¹ and R², in yields ranging from 66% to 99% (Scheme 77).¹³⁹ Interestingly, the authors showed that the reactivity switched from [2+2+2] cyclotrimerization to [4+2] cycloaddition by replacing the gold catalyst with IPrAuNTf₂ and conducting the reaction at 80 °C. These conditions allowed the formation of 1,3-diaminoisoquinolines instead of the 2,4,6-triaminopyrimidines (not shown).



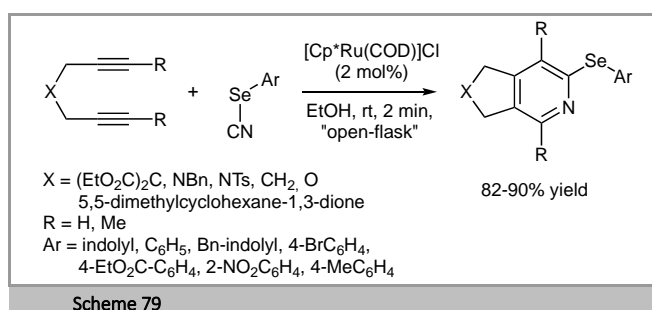
3.3. Cycloaddition of 1,6-Diynes with Selenocyanates

Considering the wide biological and pharmaceutical activities of selenium-containing heterocycles and selenopyridine derivatives, we investigated in 2019 an unexplored and straightforward method to access selenium-containing compounds. This practical route based on the

ruthenium-catalyzed [2+2+2] cycloaddition between of α,ω -diynes and aryl selenocyanates was successfully accomplished in dichloromethane or dichloroethane, at either 50 °C or 80 °C using 5 mol% of Cp*Ru(CH₃CN)₃PF₆ catalyst providing regioselectively a broad array of diaryl selenium cycloadducts containing electron-donating or -withdrawing substituents in yields up to 94%. Surprisingly, RuCl₃ and [Ru(*p*-cymene)Cl₂]₂ did not lead to the expected product (Scheme 78).¹⁴⁰

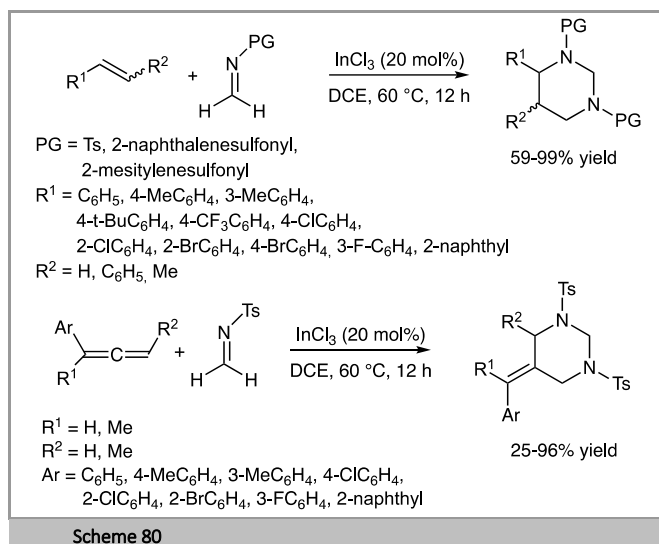


In a related study, Goswami and co-workers examined the same reaction under "open-flask" conditions, using 2 mol% of [Cp*Ru(COD)]Cl in ethanol at room temperature and a range of 2-aryl/heteroaryl selenopyridines were prepared in 82-90% yield (Scheme 79).¹⁴¹ Unsymmetrical 1,6-diynes were also employed for this cycloaddition with selenocyanates leading generally to the formation of single regioisomers (not shown).



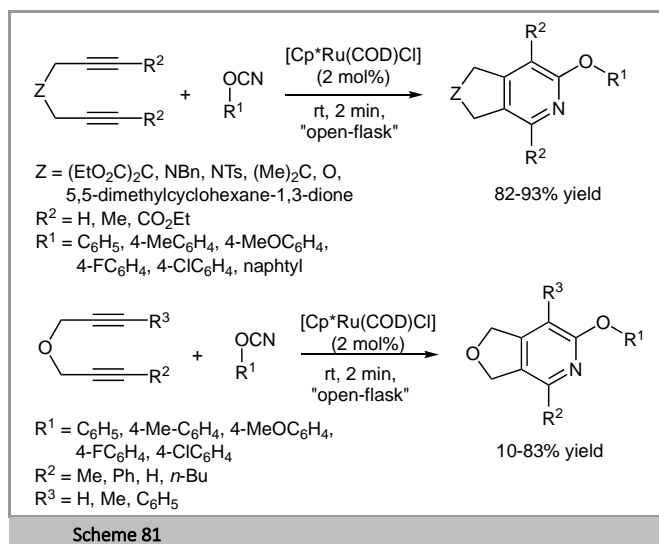
3.4. Cycloaddition of Imines with Allenes or Alkenes

Cui and co-workers developed in 2017 a practical and selective access to hexahydropyrimidines through [2+2+2] cycloaddition of alkenes or allenenes with imines. The reaction was catalyzed by InCl₃ (20 mol%) in DCE using various alkenes or allenenes with *N*-tosyl formalimine to give a range of saturated hexahydropyrimidines derivatives in yields ranging from 25% to 99% (Scheme 80).¹⁴² Based on mechanistic probing experiments, the authors suggested an "iminium-alkene-imine" addition pathway for this catalytic ionic [2+2+2] cycloaddition, that would result in the exclusive regioselectivity of the reaction with allenenes. Interestingly, acid-catalyzed hydrolysis of the hexahydropyrimidines derivatives provides a route to 1,3-diamines.



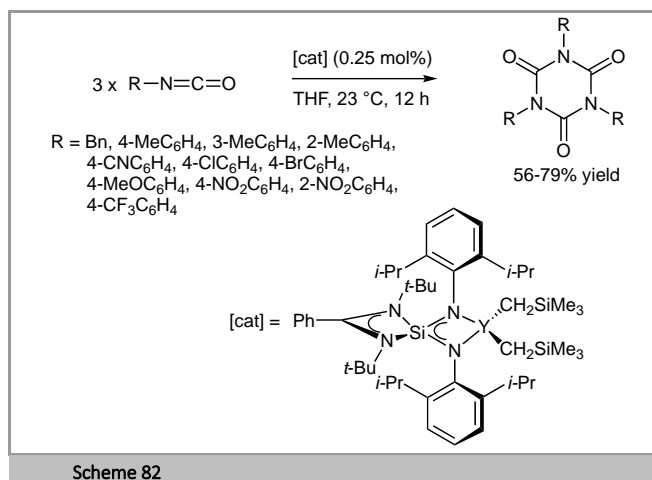
3.5. Cycloaddition of (Thio)Cyanates and Isocyanates

In 2019, Goswami and co-workers described the synthesis of 2-aryloxyppyridines by using ruthenium-catalyzed [2+2+2] cycloaddition of 1,6-diyne with aryl cyanates (Scheme 81).¹⁴³ The reaction was catalyzed by [Cp*Ru(COD)Cl] and proceeded under solvent-free conditions at room temperature with symmetrical diynes giving diversely substituted pyridines in yields ranging from 82% to 93%. On the other hand, unsymmetrical diynes furnished the desired cycloadducts as single regioisomers in 10-83% yield. Additionally, the authors extended the reaction to tetraynes which delivered the corresponding 2,2'/2,3'-diaryloxybipyridines in 78-91% yields (not shown).

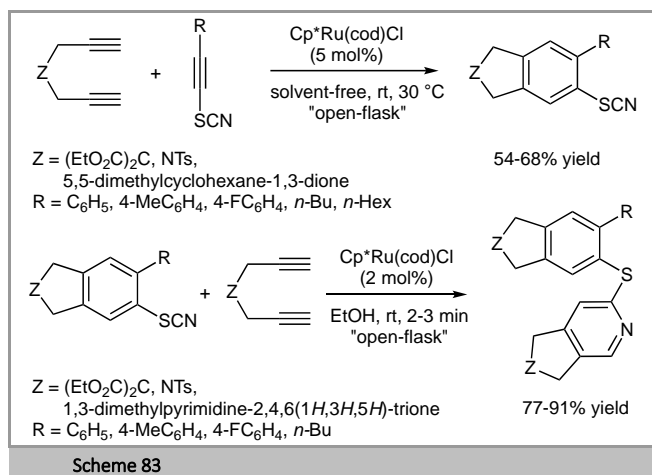


Cui, Li and co-workers developed a sterically demanding silaamidinate ligand that was used in rare-earth chemistry for the cyclotrimerization of isocyanates. The authors prepared the low-coordinate yttrium dialkyl complex [PhC(N*t*Bu)₂Si(NAr)₂Y(CH₂SiMe₃)₂] which allowed the catalytic cyclotrimerization of a range of functionalized isocyanates at room temperature and at a low catalyst loading (0.25 mol%) to

give the corresponding isocyanurates in 56-99% yield, displaying a high functional group tolerance (Scheme 82).¹⁴⁴



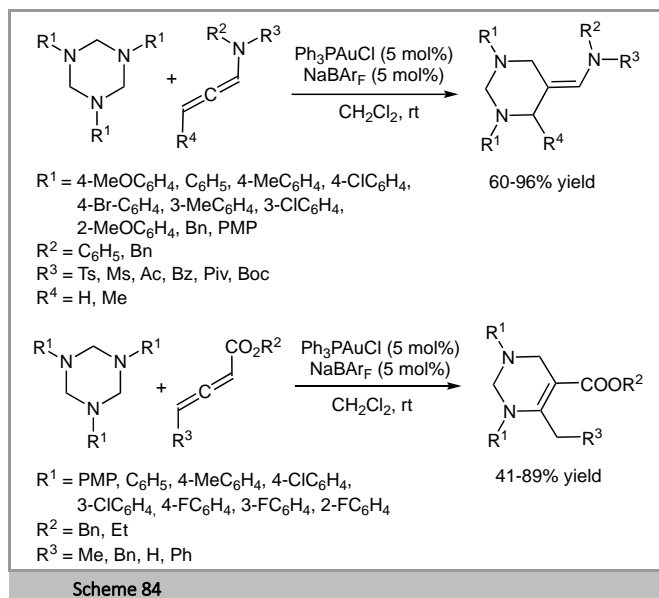
Goswami and co-workers extended their ruthenium-catalyzed [2+2+2] cycloaddition protocol that proceeds under open-flask and solvent-free conditions, to alkynylthiocyanates and 1,6-diyne for the synthesis of fused aryl thiocyanate derivatives (Scheme 83).¹⁴⁵ Whereas 1,6-heptadiyne and 1,7-octadiyne failed to afford the corresponding cyclized products, a range of symmetrical 1,6-diyne reacted chemoselectively with various alkyl- and aryl-substituted alkynylthiocyanates in the presence of [Cp*Ru(COD)Cl] in yields ranging from 54% to 68%. The authors also studied the sequential double [2+2+2] cycloaddition of these aryl thiocyanates with 1,6-diyne to access 2-aryl thiopyridines that were formed in 77-91% yield.



3.6. Cycloaddition of 1,3,5-Triazines with Allenes

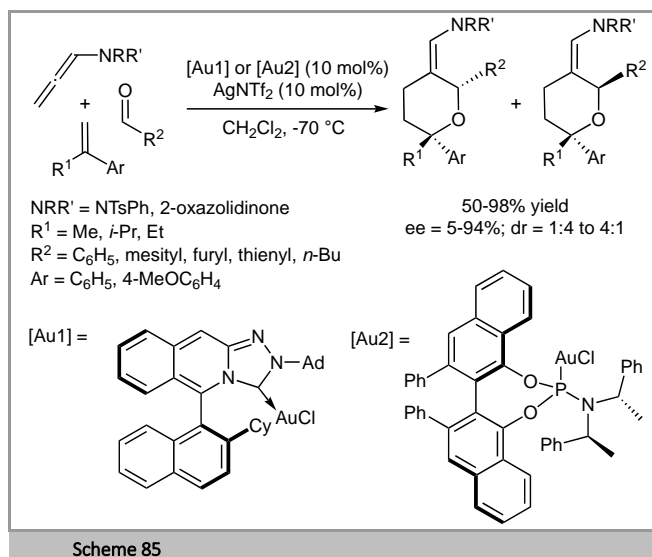
Gold-catalyzed regiodivergent [2+2+2] cycloadditions of 1,3,5-triazines with allenes were reported by Sun and co-workers in 2017 (Scheme 84).¹⁴⁶ The authors used Ph₃PAuCl/NaBAR_F (5 mol%) at room temperature in dichloromethane for the cycloaddition of substituted 1,3,5-triaryl-1,3,5-triazines with various *N*-allenamides to prepare a series of six-membered *N*-heterocycles in 60-96% yield. Interestingly, a different regioselectivity was observed when allenoids were employed instead of *N*-allenamides, affording

the cycloaddition products in 41-89% yield. Mechanistic studies including control and deuterium-labeling experiments, indicated that the formation of the six-membered *N*-heterocycles proceeded through stepwise and iterative additions of formaldimines to the allene moieties, following two distinct pathways depending on the nature of the functionalized allenes.

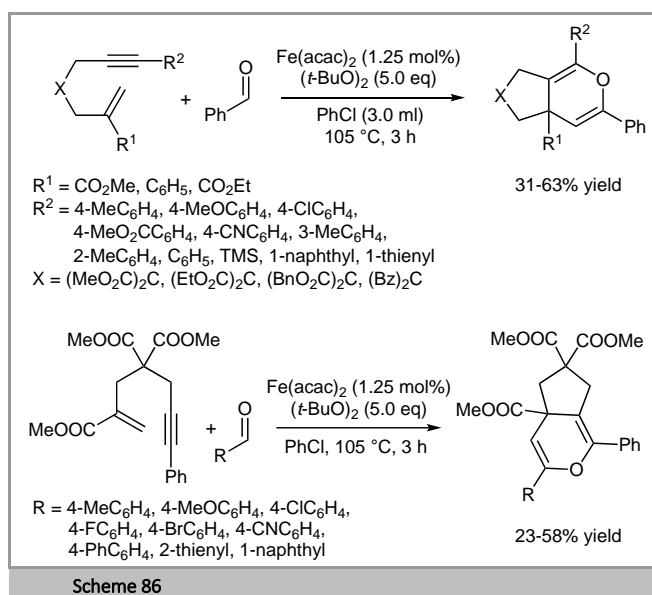


3.7. Cycloaddition of Aldehydes with Enynes or Allenes/Alkenes

In 2017, López, Mascareñas and co-workers developed a gold(I)-catalyzed enantioselective intermolecular [2+2+2] cycloaddition between allenamides, alkenes and aldehydes to prepare highly substituted tetrahydropyrans (Scheme 85).¹⁴⁷ The reaction was catalyzed by either an *N*-heterocyclic carbene- or a phosphoramidite-gold complex, [Au1] or [Au2] respectively, in the presence of AgNTf_2 in dichloromethane to afford chemo- and regioselectively the corresponding 2,6-disubstituted tetrahydropyrans which were obtained in 50-98% yield with diastereomeric ratios of >3:1 and enantioselectivities of 5-94% ee. Both 2,6-*cis* and 2,6-*trans* isomers could be obtained depending on the gold catalyst used and on the nature of the substituents on the allenamide.

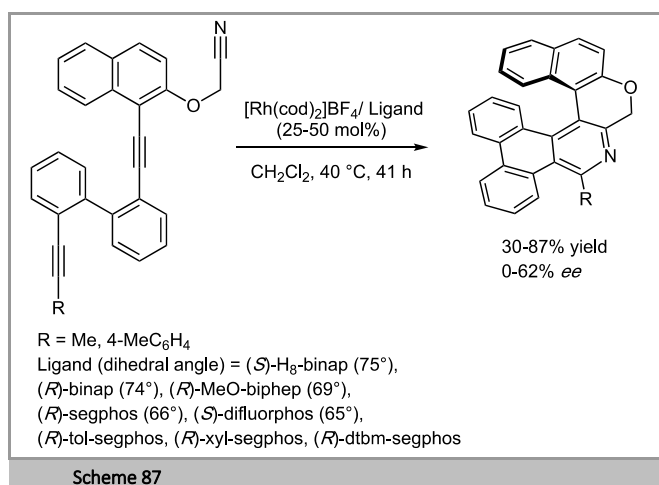


In 2020, Li and co-workers described an iron-catalyzed radical [2+2+2] annulation of aliphatic bridged 1,*n*-enynes with aldehydes to prepare fused pyrans (Scheme 86).¹⁴⁸ A large scope of 1,*n*-enynes and aldehydes having both electron-donating and electron-withdrawing groups were tolerated, delivering the functionalized fused [5.6] pyran skeletons in 23-63% yield using $\text{Fe}(\text{acac})_2$ (1.25 mol%) as the catalyst and $(t\text{-BuO})_2$ as the oxidant in PhCl at $105\text{ }^\circ\text{C}$. 1,7-Enynes were also tolerated for this reaction and afforded the corresponding isochromene derivatives (fused [6.6] pyrans) in 49-60% yield (not shown). After carrying control experiments, and based on previous reports, the authors suggested a dual role of the aldehyde partner that acts as the precursor of the acyl radical to trigger the cascade cyclization, but also as an inner-sphere radical acceptor that enables the 6-*endo-trig* cyclization of a vinyl radical.



3.8. Totally Intramolecular [2+2+2] Cycloaddition Reactions

In 2021, Tanaka and co-workers displayed an enantioselective synthesis of aza[6]helicene-like using 25-50 mol% of a cationic rhodium(I)/axially chiral biaryl bisphosphine complex catalyst. The reaction occurred at 40 °C in CH₂Cl₂ for 41 h to give the cycloadduct in 30-87% yield and ee values of 0-62%. Both yields and enantiomeric excesses were strongly dependent of the ligand. When decreasing the dihedral angle of the biaryl scaffold of the bisphosphine ligand the ee values increased. (*R*)-MeO-biphep furnished the aza[6]helicene-like in 63% yield and 53% ee in 41 h. When the reaction time was raised up to 61 h, both yield and ee increased to 73% and 53%, respectively. The use of (*S*)-difluorophos afforded the cycloadduct in 62% yield and 48% ee while (*R*)-segphos gave the product in 82% yield and 46% ee. The authors showed that increasing the steric hindrance on the phosphorus atom of segphos increased the ee value. However, no reaction was observed with (*R*)-dtbm-segphos. (*R*)-xyl-segphos was the best ligand, affording aza[6]helicene-like in 87% yield and 62% ee (Scheme 87).¹⁴⁹



4. Conclusion

This review outlines the recent developments in metal-catalyzed [2+2+2] reactions involving carbon-based π -systems to efficiently access carbocycles and heterocycles. The carbocyclization reactions reported in this review highlight inter-, partially intra- and total intramolecular cycloadditions using various organometallic complexes incorporating Rh, Ru, Ir, Pd, Co, Ni, Fe, Au, Mn, Mo, Ti, Ge, Nb, Y and In, enabling the atom-economical selective and systematic construction of polycyclic systems in a single operation. These versatile multi-component reactions allow chemo-, regio-, and stereoselective transformations and provides an efficient access to a variety of diversely functionalized products.

Acknowledgement






We thank the CNRS (Centre National de la Recherche Scientifique) and the MESRI (Ministère de l'Enseignement Supérieur, de la Recherche et de l'Innovation) for financial support. P. M. and S. H. are grateful to Chimie ParisTech for financial support.

References

- (1) (a) Berthelot, M. *Justus Liebigs Ann. Chem.* **1866**, 139, 272. (b) Berthelot, M. *C. R. Acad. Sc.* **1866**, 63, 905.
- (2) Reppe, W.; Schweckendiek, W. J. *Justus Liebigs Ann. Chem.* **1948**, 560, 104.
- (3) Hill, J. E.; Balaich, G.; Fanwick, P. E.; Rothwell, I. P. *Organometallics* **1993**, 12, 2911.
- (4) Vollhardt, K. P. C. *Angew. Chem. Int. Ed. Engl.* **1984**, 23, 539.
- (5) Ojima, I.; Tzamarioudaki, M.; Li, Z.; Donovan, R. J. *Chem. Rev.* **1996**, 96, 635.
- (6) Lautens, M.; Klute, W.; Tam, W. *Chem. Rev.* **1996**, 96, 49.
- (7) Saito, S.; Yamamoto, Y. *Chem. Rev.* **2000**, 100, 2901.
- (8) Kirchner, K.; Calhorda, M. J.; Schmid, R.; Veiros, L. F. *J. Am. Chem. Soc.* **2003**, 125, 11721.
- (9) Rubin, M.; Sromek, A. W.; Gevorgyan, V. *Synlett* **2003**, 2265.
- (10) Kotha, S.; Brahmachary, E.; Lahiri, K. *Eur. J. Org. Chem.* **2005**, 2005, 4741.
- (11) Yamamoto, Y. *Curr. Org. Chem.* **2005**, 9, 503.
- (12) Gandon, V.; Aubert, C.; Malacria, M. *Chem. Commun.* **2006**, 2209.
- (13) Tanaka, K. *Synlett* **2007**, 1977.
- (14) Agenet, N.; Buisine, O.; Slowinski, F.; Gandon, V.; Aubert, C.; Malacria, M. In *Organic Reactions*; American Cancer Society, **2007**; 1.
- (15) Hess, W.; Treutwein, J.; Hilt, G. *Synthesis* **2008**, 2008, 3537.
- (16) (a) Varela, J.; Saá, C. *Synlett* **2008**, 2008, 2571. (b) Varela, J. A.; Saá, C. *J. Organomet. Chem.* **2009**, 694, 143.
- (17) Galan, B. R.; Rovis, T. *Angew. Chem. Int. Ed.* **2009**, 48, 2830.
- (18) Pla-Quintana, A.; Roglans, A. *Molecules* **2010**, 15, 9230.
- (19) *Handbook of cyclization reactions*; Ma, S., Ed.; Wiley-VCH: Weinheim, **2010**.
- (20) Hua, R.; Victoria A. Abrenica, M.; Wang, P. *Curr. Org. Chem.* **2011**, 15, 712.
- (21) Weding, N.; Hapke, M. *Chem. Soc. Rev.* **2011**, 40, 4525.
- (22) Wang, C.; Wan, B. *Chin. Sci. Bull.* **2012**, 57, 2338.
- (23) Yamamoto, Y. In *Transition-Metal-Mediated Aromatic Ring Construction*; Tanaka, K., Ed.; John Wiley & Sons, Inc.: Hoboken, NJ, USA, **2013**; 71.
- (24) Tanaka, K. *Transition-Metal-Mediated Aromatic Ring Construction*; John Wiley & Sons, **2013**.
- (25) Kumar, P.; Louie, J. In *Transition-Metal-Mediated Aromatic Ring Construction*; Tanaka, K., Ed.; John Wiley & Sons, Inc.: Hoboken, NJ, USA, **2013**; 37.
- (26) Okamoto, S.; Sugiyama, Y. *Synlett* **2013**, 24, 1044.
- (27) Thakur, A.; Louie, J. *Acc. Chem. Res.* **2015**, 48, 2354.
- (28) Jungk, P.; Täufer, T.; Thiel, I.; Hapke, M. *Synthesis* **2016**, 48, 2026.
- (29) Sato, Y.; Nishimata, T.; Mori, M. *J. Org. Chem.* **1994**, 59, 6133.
- (30) Stará, I. G.; Starý, I.; Kollárovič, A.; Teplý, F.; Vyskočil, S.; Saman, D. *Tetrahedron Lett.* **1999**, 40, 1993.
- (31) Shibata, T.; Tsuchikama, K. *Org. Biomol. Chem.* **2008**, 6, 1317.
- (32) Tanaka, K. *Chem. Asian J.* **2009**, 4, 508.
- (33) Inglesby, P.; Evans, P. A. *Chem. Soc. Rev.* **2010**, 39, 2791.
- (34) Shibata, T.; Uchiyama, T.; Hirashima, H.; Endo, K. *Pure Appl. Chem.* **2011**, 83, 597.
- (35) Domínguez, G.; Pérez-Castells, J. *Chem. Soc. Rev.* **2011**, 40, 3430.

- (36) Marinetti, A.; Jullien, H.; Voituriez, A. *Chem. Soc. Rev.* **2012**, *41*, 4884.
- (37) Shibata, Y.; Tanaka, K. *Synthesis* **2012**, *44*, 323.
- (38) Broere, D. L. J.; Ruijter, E. *Synthesis* **2012**, *44*, 2639.
- (39) Varela, J. A.; Saá, C. *Chem. Rev.* **2003**, *103*, 3787.
- (40) Chopade, P. R.; Louie, J. *Adv. Synth. Catal.* **2006**, *348*, 2307.
- (41) D'Souza, D. M.; Müller, T. J. *Chem. Soc. Rev.* **2007**, *36*, 1095.
- (42) Heller, B.; Hapke, M. *Chem. Soc. Rev.* **2007**, *36*, 1085.
- (43) Perreault, S.; Rovis, T. *Chem. Soc. Rev.* **2009**, *38*, 3149.
- (44) Shaaban, M. R.; El-Sayed, R.; Elwahy, A. H. M. *Tetrahedron* **2011**, *67*, 6095.
- (45) Tanaka, K. *Heterocycles* **2012**, *85*, 1017.
- (46) Yamamoto, Y. *Heterocycles* **2013**, *87*, 2459.
- (47) Allais, C.; Grassot, J.-M.; Rodriguez, J.; Constantieux, T. *Chem. Rev.* **2014**, *114*, 10829.
- (48) Satoh, Y.; Obora, Y. *Eur. J. Org. Chem.* **2015**, *2015*, 5041.
- (49) Amatore, M.; Aubert, C. *Eur. J. Org. Chem.* **2015**, *2015*, 265.
- (50) Tanaka, K.; Kimura, Y.; Murayama, K. *Bull. Chem. Soc. Jpn.* **2015**, *88*, 375.
- (51) Lledó, A.; Pla-Quintana, A.; Roglans, A. *Chem. Soc. Rev.* **2016**, *45*, 2010.
- (52) Liu, Y.; Song, R.; Li, J. *Sci. China Chem.* **2016**, *59*, 161.
- (53) Domínguez, G.; Pérez-Castells, J. *Chem. Eur. J.* **2016**, *22*, 6720.
- (54) Hapke, M. *Tetrahedron Lett.* **2016**, *57*, 5719.
- (55) Yamamoto, Y. *Tetrahedron Lett.* **2017**, *58*, 3787.
- (56) Starosotnikov, A. M.; Bastrakov, M. A. *Chem. Heterocycl. Comp.* **2017**, *53*, 1181.
- (57) Babazadeh, M.; Soleimani-Amiri, S.; Vessally, E.; Hosseinian, A.; Edjlali, L. *RSC Adv.* **2017**, *7*, 43716.
- (58) Kotha, S.; Lahiri, K.; Sreevani, G. *Synlett* **2018**, *29*, 2342.
- (59) Pla-Quintana, A.; Roglans, A. *Asian J. Org. Chem.* **2018**, *7*, 1706.
- (60) Roglans, A.; Pla-Quintana, A.; Solà, M. *Chem. Rev.* **2020**, *121*, 1894.
- (61) Nagata, T.; Obora, Y. *Asian J. Org. Chem.* **2020**, *9*, 1532.
- (62) Okamoto, S.; Yamada, T.; Tanabe, Y.; Sakai, M. *Organometallics* **2018**, *37*, 4431.
- (63) Siemiaszko, G.; Six, Y. *New J. Chem.* **2018**, *42*, 2019.
- (64) Brenna, D.; Villa, M.; Gieshoff, T. N.; Fischer, F.; Hapke, M.; Jacobi von Wangelin, A. *Angew. Chem. Int. Ed.* **2017**, *56*, 8451.
- (65) Neumeier, M.; Chakraborty, U.; Schaarschmidt, D.; O'Shea, V. de la P.; Perez-Ruiz, R.; ; Jacobi von Wangelin, A. *Angew. Chem. Int. Ed.* **2020**, *59*, 13473.
- (66) Gawali, S. S.; Gunanathan, C. *J. Organomet. Chem.* **2019**, *881*, 139.
- (67) Sugahara, T.; Guo, J.-D.; Sasamori, T.; Nagase, S.; Tokitoh, N. *Angew. Chem. Int. Ed.* **2018**, *57*, 3499.
- (68) Xue, F.; Loh, Y. K.; Song, X.; Teo, W. J.; Chua, J. Y. D.; Zhao, J.; Hor, T. S. A. *Chem. Asian J.* **2017**, *12*, 168.
- (69) Kumon, T.; Yamada, S.; Agou, T.; Kubota, T.; Konno, T. *J. Fluorine Chem.* **2018**, *213*, 11.
- (70) García-Lacuna, J.; Domínguez, G.; Blanco-Urgoiti, J.; Pérez-Castells, J. *Org. Lett.* **2018**, *20*, 5219.
- (71) Ma, P.; Spencer, J. T. *Inorg. Chim. Acta.* **2018**, *482*, 67.
- (72) Jónsson, H. F.; Evjen, S.; Fiksdahl, A. *Org. Lett.* **2017**, *19*, 2202.
- (73) Tamizmani, M.; Sivasankar, C. *J. Organomet. Chem.* **2017**, *845*, 82.
- (74) Wang, Y.-I.; Hsu, W.-L.; Ho, F.-C.; Li, C.-P.; Wang, C.-F.; Chen, H.-H. *Tetrahedron* **2017**, *73*, 7210.
- (75) Weber, S. M.; Hilt, G. *Org. Lett.* **2019**, *21*, 4106.
- (76) Doll, J. S.; Eichelmann, R.; Hertwig, L. E.; Bender, T.; Kohler, V. J.; Bill, E.; Wadeppohl, H.; Roşca, D.-A. *ACS Catal.* **2021**, *11*, 5593.
- (77) Zhou, F.; Huang, Z.; Huang, Z.; Cheng, R.; Yang, Y.; You, J. *Org. Lett.* **2021**, *23*, 4559.
- (78) Nishigaki, S.; Shibata, Y.; Tanaka, K. *J. Org. Chem.* **2017**, *82*, 11117.
- (79) Reiner, B. R.; Tonks, I. A. *Inorg. Chem.* **2019**, *58*, 10508.
- (80) Silvestri, A. P.; Oakdale, J. S. *Chem. Comm.* **2020**, *56*, 13417.
- (81) Yang, K.; Wang, P.; Sun, Z.-Y.; Guo, M.; Zhao, W.; Tang, X.; Wang, G. *Org. Lett.* **2021**, *23*, 3933.
- (82) Hayase, N.; Miyauchi, Y.; Aida, Y.; Sugiyama, H.; Uekusa, H.; Shibata, Y.; Tanaka, K. *Org. Lett.* **2017**, *19*, 2993.
- (83) Alonso, J. M.; Quiroga, S.; Codony, S.; Turcu, A. L.; Barniol-Xicotá, M.; Pérez, D.; Guitián, E.; Vázquez, S.; Peña, D. *Chem. Commun.* **2018**, *54*, 5996.
- (84) Wei, S.; Yin, L.; Wang, S. R.; Tang, Y. *Org. Lett.* **2019**, *21*, 1458.
- (85) Thorve, P. R.; Guru, M. M.; Maji, B. *J. Org. Chem.* **2019**, *84*, 8185.
- (86) Ye, F.; Haddad, M.; Ratovelomanana-Vidal, V.; Michelet, V. *Catal. Commun.* **2018**, *107*, 78.
- (87) Aida, Y.; Shibata, Y.; Tanaka, K. *J. Org. Chem.* **2018**, *83*, 2617.
- (88) (a) Jeulin, S.; Duprat de Paule, S.; Ratovelomanana-Vidal, V.; Genêt, J.-P.; Champion, N.; Dellis, P. *Angew. Chem. Int. Ed.* **2004**, *43*, 320. (b) Genêt, J.-P.; Ayad, T.; Ratovelomanana-Vidal, V. *Chem. Rev.* **2014**, *114*, 2824.
- (89) Wood, J. M.; da Silva Júnior, E. N.; Bower, J. F. *Org. Lett.* **2020**, *22*, 265.
- (90) Manick, A.-D.; Salgues, B.; Parrain, J.-L.; Zaborova, E.; Fages, F.; Amatore, M.; Commeiras, L. *Org. Lett.* **2020**, *22*, 1894.
- (91) Artigas, A.; Pla-Quintana, A.; Lledó, A.; Roglans, A.; Solà, M. *Chem. Eur. J.* **2018**, *24*, 10653.
- (92) Aida, Y.; Shibata, Y.; Tanaka, K. *Chem. Asian J.* **2019**, *14*, 1823.
- (93) Maesato, T.; Shintani, R. *Chem. Lett.* **2020**, *49*, 344.
- (94) Aida, Y.; Shibata, Y.; Tanaka, K. *Chem. Eur. J.* **2020**, *26*, 3004.
- (95) Riveira, M. J.; Diez, C. M.; Mischne, M. P.; Mata, E. G. *J. Org. Chem.* **2018**, *83*, 10001.
- (96) Ni, J.; Chen, J.; Zhou, Y.; Wang, G.; Li, S.; He, Z.; Sun, W.; Fan, B. *Adv. Synth. Catal.* **2019**, *361*, 3543.
- (97) Teng, Q.; Mao, W.; Chen, D.; Wang, Z.; Tung, C.-H.; Xu, Z. *Angew. Chem. Int. Ed.* **2020**, *59*, 2220.
- (98) Suzuki, S.; Shibata, Y.; Tanaka, K. *Chem. Eur. J.* **2020**, *26*, 3698.
- (99) Agou, T.; Saruwatari, S.; Shirai, T.; Kumon, T.; Yamada, S.; Konno, T.; Mizuhata, Y.; Tokitoh, N.; Sei, Y.; Fukumoto, H.; Kubota, T. *J. Fluorine Chem.* **2020**, *234*, 109512.
- (100) Rycek, L.; Mateus, M.; Beytlerová, N.; Katora, M. *Org. Lett.* **2021**, *23*, 4511.
- (101) Kotha, S.; Sreevani, G. *Synthesis* **2018**, *50*, 4883.
- (102) Kotha, S.; Sreevani, G. *Eur. J. Org. Chem.* **2018**, *2018*, 5935.
- (103) Xu, F.; Si, X.-J.; Wang, X.-N.; Kou, H.-D.; Chen, D.-M.; Liu, C.-S.; Du, M. *RSC Adv.* **2018**, *8*, 4895.
- (104) Kumon, T.; Yamada, S.; Agou, T.; Kubota, T.; Konno, T. *J. Fluorine Chem.* **2018**, *213*, 11.
- (105) Méndez-Gálvez, C.; Böhme, M.; Leino, R.; Savela, R. *Eur. J. Org. Chem.* **2020**, *2020*, 1708.

- (106) Amakasu, T.; Sato, K.; Ohta, Y.; Kitazawa, G.; Sato, H.; Oumiya, K.; Kawakami, Y.; Takeuchi, T.; Kabe, Y. *J. Organomet. Chem.* **2020**, *905*, 121006.
- (107) Aechtner, T.; Barry, D. A.; David, E.; Ghellamallah, C.; Harvey, D. F.; de la Houpliere, A.; Knopp, M.; Malaska, M. J.; Pérez, D.; Schärer, K. A.; Siesel, B. A.; Vollhardt, K. P. C.; Zitterbart, R. *Synthesis* **2018**, *50*, 1053.
- (108) Caivano, I.; Kaiser, R. P.; Schnurrer, F.; Mosinger, J.; Císařová, I.; Nečas, D.; Kotora, M. *Catalysts* **2019**, *9*, 942.
- (109) Tan, J.-F.; Bormann, C. T.; Perrin, F. G.; Chadwick, F. M.; Severin, K.; Cramer, N. *J. Am. Chem. Soc.* **2019**, *141*, 10372.
- (110) Liu, R.; Giordano, L.; Tenaglia, A. *Chem. Asian J.* **2017**, *12*, 2245.
- (111) Petko, D.; Pounder, A.; Tam, W. *Synthesis* **2019**, *51*, 4271.
- (112) Miguel-Ávila, J.; Tomás-Gamasa, M.; Mascareñas, J. L. *Angew. Chem. Int. Ed.* **2020**, *59*, 17628.
- (113) Miura, H.; Tanaka, Y.; Nakahara, K.; Hachiya, Y.; Endo, K.; Shishido, T. *Angew. Chem. Int. Ed.* **2018**, *57*, 6136.
- (114) Watanabe, K.; Satoh, Y.; Kamei, M.; Furukawa, H.; Fujii, M.; Obora, Y. *Org. Lett.* **2017**, *19*, 5398.
- (115) Sawano, T.; Toyoshima, Y.; Takeuchi, R. *Inorganics* **2019**, *7*, 138.
- (116) Arai, S.; Izaki, A.; Amako, Y.; Nakajima, M.; Uchiyama, M.; Nishida, A. *Adv. Synth. Catal.* **2019**, *361*, 4882.
- (117) Zhao, W.-C.; Wang, X.; Feng, J.; Tian, P.; He, Z.-T. *Tetrahedron* **2021**, *79*, 131862.
- (118) Mitake, A.; Fusamae, T.; Kanyiva, K. S.; Shibata, T. *Eur. J. Org. Chem.* **2017**, *2017*, 7266.
- (119) Shibata, T.; Fusamae, T.; Takano, H.; Sugimura, N.; Kanyiva, K. S. *Asian J. Org. Chem.* **2019**, *8*, 970.
- (120) Kimura, Y.; Shibata, Y.; Tanaka, K. *Chem. Lett.* **2018**, *47*, 806.
- (121) Nishigaki, S.; Shibata, Y.; Nakajima, A.; Okajima, H.; Masumoto, Y.; Osawa, T.; Muranaka, A.; Sugiyama, H.; Horikawa, A.; Uekusa, H.; Koshino, H.; Uchiyama, M.; Sakamoto, A.; Tanaka, K. *J. Am. Chem. Soc.* **2019**, *141*, 14955.
- (122) Aida, Y.; Nogami, J.; Sugiyama, H.; Uekusa, H.; Tanaka, K. *Chem. Eur. J.* **2020**, *26*, 12579.
- (123) Yasui, T.; Nakazato, Y.; Kurisaki, K.; Yamamoto, Y. *Adv. Synth. Catal.* **2021**, DOI: 10.1002/adsc.202100513.
- (124) Cadart, T.; Nečas, D.; Kaiser, R. P.; Favereau, L.; Císařová, I.; Gyepes, R.; Hodačova, J.; Kalikova, K.; Bednarova, L.; Crassous, J.; Kotora, M. *Chem. Eur. J.* **2021**, DOI: 10.1002/chem.202100759.
- (125) Trommer, V.; Fischer, F.; Hapke, M. *Monatsh. Chem.* **2018**, *149*, 755.
- (126) Bhatt, D.; Patel, N.; Chowdhury, H.; Bharatam, P. V.; Goswami, A. *Adv. Synth. Catal.* **2018**, *360*, 1876.
- (127) Murayama, K.; Shibata, Y.; Sugiyama, H.; Uekusa, H.; Tanaka, K. *J. Org. Chem.* **2017**, *82*, 1136.
- (128) Xie, Y.; Wu, C.; Jia, C.; Tung, C.-H.; Wang, W. *Org. Chem. Front.* **2020**, *7*, 2196.
- (129) Li, K.; Wei, L.; Sun, M.; Li, B.; Liu, M.; Li, C. *Ang. Chem. Int. Ed.* **2021**, doi: 10.1002/anie.202105452.
- (130) Kumon, T.; Yamada, S.; Agou, T.; Fukumoto, H.; Kubota, T.; Hammond, G. B.; Konno, T. *Adv. Synth. Catal.* **2021**, *363*, 1912.
- (131) Cho, I. Y.; Kim, W. K.; Ji, J. H.; Lee, J. W.; Seo, J. K.; Seo, J.; Hong, S. Y. *J. Org. Chem.* **2021**, DOI: 10.1021/acs.joc.1c00577.
- (132) Wang, C.-S.; Sun, Q.; García, F.; Wang, C.; Yoshikai, N. *Angew. Chem. Int. Ed.* **2021**, *60*, 9627.
- (133) Ye, F.; Haddad, M.; Michelet, V.; Ratovelomanana-Vidal, V. *Org. Chem. Front.* **2017**, *4*, 1063.
- (134) Ye, F.; Haddad, M.; Ratovelomanana-Vidal, V.; Michelet, V. *Org. Lett.* **2017**, *19*, 1104.
- (135) Ye, F.; Boukattaya, F.; Haddad, M.; Ratovelomanana-Vidal, V.; Michelet, V. *New J. Chem.* **2018**, *42*, 3222.
- (136) Ye, F.; Tran, C.; Jullien, L.; Le Saux, T.; Haddad, M.; Michelet, V.; Ratovelomanana-Vidal, V. *Org. Lett.* **2018**, *20*, 4950.
- (137) Tran, C.; Haddad, M.; Ratovelomanana-Vidal, V. *Synlett* **2019**, *30*, 1891.
- (138) Medas, K. M.; Lesch, R. W.; Idioma, F. B.; Wrenn, S. P.; Ndahayo, V.; Mulcahy, S. P. *Org. Lett.* **2020**, *22*, 3135.
- (139) Dubovtsev, A. Y.; Shcherbakov, N. V.; Dar'in, D. V.; Kukushkin, V. Y. *Adv. Synth. Catal.* **2020**, *362*, 2672.
- (140) Tran, C.; Haddad, M.; Ratovelomanana-Vidal, V. *Synthesis* **2019**, *51*, 2532.
- (141) Kalaramma, P.; Bhatt, D.; Sharma, H.; Goswami, A. *Eur. J. Org. Chem.* **2019**, *2019*, 4694.
- (142) Zhou, H.; Chaminda Lakmal, H. H.; Baine, J. M.; Valle, H. U.; Xu, X.; Cui, X. *Chem Sci* **2017**, *8*, 6520.
- (143) Kalaramma, P.; Bhatt, D.; Sharma, H.; Goswami, A. *Adv. Synth. Catal.* **2019**, *361*, 4379.
- (144) Liu, D.; Zhou, D.; Yang, H.; Li, J.; Cui, C. *Chem. Commun.* **2019**, *55*, 12324.
- (145) Bhatt, D.; Kalaramma, P.; Kumar, K.; Goswami, A. *Eur. J. Org. Chem.* **2020**, *2020*, 4606.
- (146) Peng, S.; Cao, S.; Sun, J. *Org. Lett.* **2017**, *19*, 524.
- (147) Varela, I.; Faustino, H.; Díez, E.; Iglesias-Sigüenza, J.; Grande-Carmona, F.; Fernández, R.; Lassaletta, J. M.; Mascareñas, J. L.; López, F. *ACS Catal.* **2017**, *7*, 2397.
- (148) Tian, T.; Wang, X.; Lv, L.; Li, Z. *Eur. J. Org. Chem.* **2020**, *2020*, 4425.
- (149) Hanada, K.; Nogami, J.; Miyamoto, K.; Hayase, N.; Nagashima, Y.; Tanaka, Y.; Muranaka, A.; Uchiyama, M.; Tanaka, K. *Chem. Eur. J.* **2021**, DOI: doi.org/10.1002/chem.202100759.

	<p>Virginie Vidal was born in Paris (France). She completed her PhD at Paris-Sud University under the supervision of Prof. H.P. Husson and Dr. J. Royer (Gif, France) and was a FRM post-doctoral fellow at the University of Montreal with Prof. S. Hanessian (Canada, 1989-1990), and in 1991 with Prof. P. Potier and Dr. R. H. Dodd (Gif). She was appointed as a CNRS Associate Researcher with Prof. J. P. Genêt at Ecole Nationale Supérieure de Chimie de Paris. She is currently CNRS Research Director at Chimie ParisTech (Paris, France). Her research interests focus on the development of transition-metal catalysis and the design of atropisomeric ligands (Synphos and Difluorphos). The synthesis of biorelevant targets is also a focus in her research group. She was Chair of the Division of Organic Chemistry of the French Chemical Society (2009–2012).</p>
	<p>Phannarath Phansavath was born in Vientiane (Laos). She received her PhD from Pierre & Marie Curie University in 1997 under the supervision of Prof. M. Malacria and Dr C. Aubert. After postdoctoral studies in the group of Prof. C. Bolm at the Institut für Organische Chemie, RWTH Aachen (Germany), she was appointed assistant professor in 1999 in the group of Prof. J.-P. Genêt at Ecole Nationale Supérieure de Chimie de Paris (Chimie ParisTech). Her current research interests include total synthesis of biologically relevant natural products and transition metal-catalyzed asymmetric reactions.</p>
	<p>Mansour Haddad was born in 1958 at Homs (Syria). He received his PhD from Pierre & Marie Curie University in 1986 under the supervision of Prof. G. Lhomme. He was appointed as a CNRS Associate Researcher in 1989 and worked on fluorine chemistry. He joined the group of Prof. J.-P. Genêt at Ecole Nationale Supérieure de Chimie de Paris (Chimie ParisTech) in 1994 and was involved in asymmetric total synthesis of nitrogen-containing heterocycles. Since 2013, he is involved in metal-catalyzed [2+2+2] cycloaddition reaction.</p>
	<p>Steve Huvelle was born in 1989 in France. He graduated from Paris Diderot University (Paris, France) in 2014. He received his PhD. from PSL University under the supervision of Dr F. Schmidt (Curie Institute, France). During this time, his research focused on self-immolative spacers and their applications in chemical biology. After post-doctoral studies with Prof. M-C. Viaud-Massuard working on antibody-drug conjugates, he moved to ENSCP Chimie ParisTech in 2020 as a post-doctoral associate in the research group of Dr V. Vidal. His current research fields include metal-catalyzed [2+2+2] cycloaddition reactions.</p>
	<p>Pascal Matton was born in 1988 in France. He graduated from the Engineering School ESCOM (Compiègne, France) and UPMC. He received his PhD from ENS-Ulm (Paris) in 2017 under the supervision of Dr J.-M. Mallet and Dr J. Fattaccioni, working on the synthesis of glycolipids, the fabrication of functionalized oil droplets and their interaction with lectins. He joined the research group of Dr V. Vidal as a postdoctoral associate, working on [2+2+2] cycloaddition (2019-2020), then the group of Prof. C. Thomas to work on biobased polymers (2020-2021).</p>